Biogeosciences Discuss., doi:10.5194/bg-2016-144, 2016
Manuscript under review for journal Biogeosciences
Published: 21 April 2016

Paleohydrological changes over the last 50 ky in the central Gulf of Cadiz: Complex forcing mechanisms mixing multi-scale processes

PENAUD Aurélie [(a)] ***, EYNAUD Frédérique** [(b)]

VOELKER Antje Helga Luise [(c,d)]**, TURON Jean-Louis** [(b)]

(a) Univ Brest, CNRS, UMR 6538 Domaines Océaniques, IUEM, 29280, Plouzané, France.

(b) Univ Bordeaux, CNRS, UMR 5805 EPOC, Allée Geoffroy St Hilaire, 33615, Pessac, France.

(c) Divisão de Geologia e Georecursos Marinhos, Instituto Português do Mar e da Atmosfera (IPMA), Rua Alfredo Magalhães Ramalho 6, 1495-006 Lisboa, Portugal

(d) CCMAR, Centro de Ciencias do Mar, Universidade do Algarve, Campus de Gambelas, 8005-139 Faro, Portugal

*Corresponding author.
Tel.: +33-298-498-741; fax: +33-298-498-760.
E-mail address: aurelie.penaud@univ-brest.fr.

Biogeosciences Discuss., doi:10.5194/bg-2016-144, 2016
Manuscript under review for journal Biogeosciences
Published: 21 April 2016

ABSTRACT

New dinoflagellate cyst (dinocyst) analyses were carried out at high-resolution in core MD99-2339, retrieved from a contouritic field in the central part of the Gulf of Cadiz, for the Marine Isotope Stage (MIS) 3 interval, allowing to discuss paleohydrological changes over the last 50 ky in the subtropical NE Atlantic Ocean. Some index dinocyst taxa, according to their (paleo) ecological significance, shed light on significant sea-surface changes. Superimposed on the general decreasing pattern of dinocyst export to the seafloor over the last 50 ky, paralleling the general context of decreasing aeolian dust fertilization, a complex variability in dinocyst assemblages was detected at millennial timescale. Enhanced fluvial discharges occurred during Greenland Interstadials (GI) and especially GI 1, 8 and 12, while enhanced upwelling cell dynamics were suggested during the Last Glacial Maximum and Heinrich Stadials. Finally, during the early Holocene, and more specifically during the Sapropel 1 interval (around 7-9 ka BP), we evidenced a strong decrease in dinocyst fluxes, which occurred synchronously to a strong reduction in Mediterranean Outflow Water strength, and that we attributed to an advection of warm and nutrient-poor subtropical North Atlantic Central Waters. Over the last 50 ky, our study thus allows capturing and documenting the fine tuning existing between terrestrial and marine realms in North Atlantic subtropical latitudes, not only in response to the regional climate pattern, but also to monsoonal forcing interfering during precession-driven northern hemisphere insolation maxima. This mechanism, well expressed during the Holocene, is superimposed on the pervasive role of the obliquity as a first major trigger for explaining migration of dinocyst productive centres in the NE Atlantic margin to the subtropical (temperate) latitudes during glacial (interglacial) periods.

KEYWORDS: Gulf of Cadiz; Dinoflagellate cysts; Dansgaard-Oeschger events; Lingulodinium machaerophorum; Obliquity and precession forcing; Paleoriver discharges; Upwellings.

Biogeosciences Discuss., doi:10.5194/bg-2016-144, 2016
Manuscript under review for journal Biogeosciences
Published: 21 April 2016

1. INTRODUCTION

At present, ocean and land biospheres act as major sinks for anthropogenic carbon emissions to the atmosphere (e.g. Sarmiento and Gruber, 2002), compensating for approximately half of its additional effect with respect to natural greenhouse gas trends (Sabine et al., 2004). In this context, the North Atlantic is the major contributor to atmospheric CO_2 sequestration (Sabine et al., 2004; Takahashi et al., 2009), especially in high latitudes. Marginal and semi-enclosed seas, as well as continental shelves, also significantly contribute to CO_2 storage, even if uncertainties remain on the calculated amount stored by these coastal regions (e.g. Flecha et al., 2012). Disregarding abiotic processes, CO_2 storage evolution is itself substantially governed by continental and marine primary producers through carbon biological fixing, export and fossilization. The majority of ocean primary production comes from microphytoplanktonic organisms (mostly diatoms, coccolithophores and dinoflagellates; Falkowski and Raven, 1997), mainly in coastal upwelling systems as well as in temperate and subpolar regions; these micro-organisms being extremely sensitive to climate changes at seasonal and interannual time scales. In this study, we targeted a major component of the modern phytoplanktonic biomass, the dinoflagellate group. About 15% of living dinoflagellate species form highly resistant resting cysts (dinocysts) after sexual reproduction (Dodge and Harland, 1991; Head, 1996; Dale, 1996) whose modern distribution is tightly coupled to sea-surface physico-chemical characteristics (nutrient availability, temperature, salinity or light penetration; Rochon et al., 1999; Marret and Zonneveld, 2003; de Vernal et al., 2001, 2005; de Vernal and Marret, 2007; Zonneveld et al., 2013). Dinocysts recorded in marine sediments thus enable to discuss qualitatively as well as quantitatively past surface environments; their preservation being furthermore high in comparison to other fossilisable planktonic groups suffering from dissolution issues of authigenic silica and carbonates (e.g. de Leeuw et al., 2006).

Biogeosciences Discuss., doi:10.5194/bg-2016-144, 2016
Manuscript under review for journal Biogeosciences
Published: 21 April 2016

Here, new dinocyst data have been acquired in a sediment core retrieved from the central Gulf of Cadiz in a context of present-day low productive surface waters, as deduced from carbon uptake quantifications which demonstrated that the Gulf of Cadiz is today moderately responsible for CO_2 storage (e.g. Huertas et al., 2006, 2009; Flecha et al, 2012). However, this may have been different in the past considering the potential migration of proximal productive centres (e.g. Moroccan and Portuguese upwellings) through time at long-term orbital timescales (glacial-interglacial cycles) as well as at millennial sub-orbital ones (i.e. the well-known Greenland Interstadial (GI) / Greenland Stadial (GS) cycles; Dansgaard et al., 1993; Grootes et al., 1993). Actually, it was demonstrated that productivity changes in our study area involve complex hydrographical dynamics, including upwelling, river inputs, also probably additionally forced by Mediterranean-Atlantic exchanges (Rogerson et al., 2012; Ivanovic et al., 2013). Our study thus intends to focus on the response of dinoflagellates, here viewed as an index planktonic group, so as to understand complex patterns and couplings of paleohydrological and paleoproductivity changes over the last 50 ky in the subtropical NE Atlantic. Large environmental shifts which have characterized the studied period are known to be well expressed and preserved in the Gulf of Cadiz sedimentological archives (e.g. Sierro et al., 2005; Voelker et al., 2006, 2015; Toucanne et al., 2007; Peliz et al., 2009; Rogerson et al., 2010, 2012; Bahr et al., 2014, 2015; Hernandez-Molina et al., 2014), thus providing an ideal case study for our purposes. Different configurations of Mediterranean-Atlantic exchanges were also taken into account regarding their potential impacts on MD99-2339 dinocyst surface proxies. We also considered the Northern Hemisphere paleoclimatological changes within a broader subtropical context, including the Mediterranean Basin.

Biogeosciences Discuss., doi:10.5194/bg-2016-144, 2016
Manuscript under review for journal Biogeosciences
Published: 21 April 2016

2. SURFACE AND DEEP HYDROGRAPHYOF THE GULF OF CADIZ

The study area is focussed on the oriental part of the North Atlantic subtropical gyre directly adjacent to the Gibraltar Strait (<14km width, <300m depth); the latter channelling water mass exchanges between Atlantic waters at the surface and saltier/denser Mediterranean Outflow Waters (MOW) at depth. This area thus associates the convergence of critical water masses regarding the Atlantic Meridional Overturning Circulation (AMOC) with a semi-permanent upwelling regime, itself connected to the larger dynamic cells off NW Africa.

More specifically, sea-surface waters from the Gulf of Cadiz are influenced by several features which are: the Portuguese and Moroccan coastal currents, a branch of the Azores Current (AzC; Figure 1) flowing eastward at 35°N (Rogerson et al., 2004), and the MOW also contributing to the generation of the AzC that feeds the Canary Current (CC; Figure 1) to the South. In the open ocean only, the AzC coincides with the Azores Front (AF), forming a strong hydrographical barrier at the northeastern boundary of the Atlantic subtropical gyre marked both in terms of temperature gradients (about 4°C; Gould, 1985) and vertical structure of the water column (Fasham et al., 1985). This front is locally characterized by intense upwelling cells and thus higher sea-surface productivity (Rudnick, 1996; Alves and DeVerdière, 1999; Alves et al., 2002). Nowadays, the AF does not penetrate into the Gulf of Cadiz where sea-surface waters are generally depleted in nutrients. Total chlorophyll values and primary production rates found in the area over the upper 50 m are typical of those reported for oligotrophic environments (Navarro and Ruiz, 2006). The Gulf of Cadiz is thus today moderately responsible for CO_2 storage (e.g. Huertas et al., 2006, 2009; Flecha et al, 2012), and this oligotrophic regime is mainly due to surface inflow of relatively nutrient-depleted Atlantic water, while nutrient-richer conditions are found at depth as a consequence of the MOW outflow.

On the north-eastern shelf of the Gulf of Cadiz, it has been demonstrated that present-day river discharges (freshwater inputs from large rivers such as the Guadania, Tinto-Odiel and especially

Biogeosciences Discuss., doi:10.5194/bg-2016-144, 2016
Manuscript under review for journal Biogeosciences
Published: 21 April 2016

117 the Guadalquivir on the southern Iberian margin), in combination with meteorological conditions
118 (incident irradiance, strong winds), strongly impact phytoplankton biomass (Huertas et al., 2006).
119 More specifically, turbidity plume and chlorophyll concentration dynamics shed light on
120 enhanced primary productivity conditions related to fluvial discharges occurring during rainy
121 seasons, and especially during negative modes of the North Atlantic Oscillation (NAO)
122 (Caballero et al., 2014). The central Gulf of Cadiz is, conversely, rather subject to fluvial
123 influences from NW Moroccan rivers (especially from the Sebou River and additional northern
124 African small distributaries) for which plumes spread over a large coastal area (Warrick and
125 Fong, 2004). Additionally, the wind pattern is highly significant for sea-surface biological
126 processes within the Gulf of Cadiz (Navarro and Ruiz, 2006): the wind-related mixing
127 phenomenon cumulates with the wind-driven coastal upwelling regime, active mainly from late
128 May / early June to late September / early October in the Portugal-Canary system (e.g. Haynes et
129 al., 1993; Aristegui et al., 2005; Peliz et al., 2005). This seasonal upwelling functioning is itself
130 dependent on seasonal migrations of the Azores High coupled to the Intertropical Convergence
131 Zone dynamics (Hsu and Wallace, 1976). Over the last 30 ky, the evidence of extremely close
132 paleohydrological patterns between the central Gulf of Cadiz and the NW Moroccan margin
133 supported the idea of similar forcing acting on both these subtropical areas of the NE Atlantic
134 margin (Penaud et al., 2011a).
135 Water masses from our study area are structured as follow: Surface Atlantic Waters, between the
136 surface and 100 m water depth, overlay North Atlantic Central Waters, found between 100 and
137 700m. Deep MOW are divided into two main branches centred at around 800 and 1,200 m water
138 depths, and also at 500 m in the continental shelf (Ambar and Howe, 1979; Ambar et al., 2002).
139 North Atlantic Deep Waters are found below 1,500 m (Alvarez et al., 2005).
140

Biogeosciences Discuss., doi:10.5194/bg-2016-144, 2016
Manuscript under review for journal Biogeosciences
Published: 21 April 2016

3. MATERIAL AND METHODOLOGY

3.1. Marine cores integrated within the study: chrono-stratigraphy

The central sequence of this manuscript, core MD99-2339 (35.89°N; 7.53°W; 1170m water depth; 18.54m length; Figure 1), was recovered in a contouritic field (Habgood et al., 2003) by the R/V Marion Dufresne during the 1999 International Marine Global Change Studies V (IMAGES V-GINNA) cruise (Labeyrie, Jansen and Cortijo, 2003). It covers the last 45 ky according to its published age model (Voelker et al., 2006): 20 AMS ^{14}C dates and three δ^{18}O control points tuned with the GISP2 chronology (Grootes and Stuiver, 1997).

In this study, the stratigraphical framework of core MD99-2339 was re-considered for its older part, where radiocarbon dates exhibited large error bars (between 200 years around 900cm and 1,400 years at 1500cm; Voelker et al., 2006; Figure 3) and inconsistencies with the regional North Atlantic stratotype NGRIP (GICC05 timescale; Svensson et al., 2008; Austin et al., 2012; Austin and Hibbert, 2012). This revision was furthermore motivated by the comparison of this new dinocyst MIS 3 record to that of core MD95-2043 (Alboran Sea; 36.14 °N; 2.62°W; 1841m water depth; 36m length; Penaud et al., 2011b; Figure 1). To build the revised age model (Figure 2), we chose to keep 6 radiocarbon dates (Voelker et al., 2006; Figure 3) younger than 20 ka BP (until around 600-700cm; mean errors of 60 years) that we calibrated to calendar years with the CALIB 7.1 program (Marine13 calibration; Stuiver and Reimer, 1993). We also tuned planktonic monospecific δ^{18}O data (*G. bulloides*) of core MD99-2339 (13 pointers; Figures 2 and 3) to NGRIP (GICC05 timescale), considering synchronous sea-surface warmings in the Gulf of Cadiz with the onset of GI 3 to 12 (Wolff et al., 2010). As a result, Heinrich Stadial (HS, Barker et al., 2009; Sanchez-Goni and Harrison, 2010) 5 (HS5) is dated around 48 ka BP in our revised age model rather than 45-46 ka BP (Voelker et al., 2006; Figure 3). Sedimentation rates show a

Biogeosciences Discuss., doi:10.5194/bg-2016-144, 2016
Manuscript under review for journal Biogeosciences
Published: 21 April 2016

164 general decreasing trend from 60-90 cm/ka around 40-45 ka BP to 10-40 cm/ka across the
165 Holocene (Figure 2).
166
167 ***3.2 Dinoflagellate cyst (dinocyst) analysis***
168 *3.2.1. Laboratory procedure and microscopic observation*
169 Dinocyst assemblages were characterized in the fraction 10-150 µm on 161 palynological slides
170 (every 10 cm in average, representing a sample resolution of around 300 years [σ=210]) for the
171 whole MD99-2339 sequence, using an Olympus BX50 microscope at 400X magnification (75
172 slides from 0 to 740 cm / 0 to 27 ka BP: Penaud et al., 2011a; 86 slides from 750 to 1844 cm / 27
173 to 49 ka BP: this study). The preparation technique followed the protocol described by de Vernal
174 et al. (1999) and Rochon et al. (1999), slightly modified at the EPOC laboratory (Castera and
175 Turon, http://www.epoc.u-bordeaux.fr/index.php?lang=fr&page=eq_paleo_pollens), including
176 chemical treatments (cold HCl and HF) and sieving through single-use 10µm nylon mesh
177 screens. The final residue was then mounted between slide and coverslip with glycerine jelly
178 coloured with fushin.
179 For each analysed sample, a minimum of 300 dinocyst specimens were systematically identified
180 following Fensome and Williams (2004) and Fensome et al. (2008), and represented thanks to
181 species percentages excluding reworked (non Quaternary) specimens and non-identified taxa.
182 High occurrences of the species *Lingulodinium machaerophorum* (nearly monospecific in some
183 cases but typical for the area today) forced us to additionally count 100 dinocysts outside this
184 species for each palynological slide to obtain statistically robust dinocyst results (Fatela and
185 Taborda, 2002).
186 Dinocysts can also be expressed in concentrations (number of specimens/cm^3 of dry sediments),
187 that are calculated through the marker grain method (Stockmarr, 1971; de Vernal et al., 1999;
188 Mertens et al., 2009a). This consists in adding aliquot volumes of *Lycopodium* spores before the

Biogeosciences Discuss., doi:10.5194/bg-2016-144, 2016
Manuscript under review for journal Biogeosciences
Published: 21 April 2016

189 palynological treatment in each sample; these exotic spores being counted in parallel with fossil
190 palynomorphs. One can argue that there might be a relationship between concentrations and
191 granulometry (increasing / decreasing concentrations *versus* increasing clays-fine silts / coarser
192 silts-fine sands) (Wall et al., 1977), especially in a contouritic environment. However, it is
193 important to note that only fine silts have been sampled for palynological analysis. Furthermore,
194 given that cyst concentrations are the combined results of sedimentation rates, grain-size and
195 productivity, we also calculated flux rates (number of cysts/cm^2/ka). We do not have enough time
196 marker points to calculate flux rates for every single short event separately, but at least on a
197 multi-millennial timescale, dinocyst fluxes may provide a better insight on dinocyst export to the
198 seafloor, and perhaps also indirectly on dinoflagellate productivity in surface waters.
199
200 *3.2.2. Dinocyst indexes and Statistical treatments of dinocyst results*
201 ***Warm / Cold ratio***
202 The present-day ecology of many of the recovered species is well known from their surface
203 sediment distribution in the North Atlantic (e.g. Turon, 1984; Rochon et al., 1999). Furthermore,
204 latitudinal (SST changes) and inshore-offshore (eutrophic-oligotrophic conditions) gradients are
205 mainly responsible for dinocyst distribution in modern sediments (Marret and Zonneveld, 2003;
206 Zonneveld et al., 2013). A qualitative thermic index "Warm/Cold" (W/C) has previously been
207 used (Turon and Londeix, 1988; Versteegh, 1994; Combourieu-Nebout et al., 1999; Eynaud et
208 al., 2016) to address qualitatively SST change issues. We also calculated a W/C ratio for MD99-
209 2339 core (cf. Table 1 for the species grouped in this thermophilic ratio).
210
211 ***Heterotrophic / Autotrophic ratio***
212 Most dinoflagellate species are mixotrophic, and strict autotrophic (phototrophic organisms) are
213 rare. However, previous investigations discussed heterotrophic cysts, i.e. derived from

Biogeosciences Discuss., doi:10.5194/bg-2016-144, 2016
Manuscript under review for journal Biogeosciences
Published: 21 April 2016

dinoflagellates with a strict heterotrophic strategy of nutrition, as being indirectly related to food resources, and especially diatoms, as it has commonly been shown in upwelling areas (Wall et al., 1977; Lewis et al., 1990; Marret, 1994; Biebow, 1996; Zonneveld et al., 1997a, 2001; Targarona et al., 1999; Bouimetarhan et al., 2009; Penaud et al., 2011a). This is especially true for Protoperidinium species, including *Brigantedinium* and *Selenopemphix* species, thus indirectly signing periods of higher surface water productivity. In the following sections of the paper, we will refer these taxa as "heterotrophics"; "coastal heterotrophics" being more specifically used for *Selenopemphix* species (*S. quanta* and *S. nephroides*; Table 1). Also a ratio "Hetrotrophics / Autototrophics" (H/A) can be addressed that simply takes into account "strict" heterotrophics occurrences *versus* the other dinocyst taxa identified in fossil assemblages.

Diversity statistics

Quantifying taxonomical diversity in study samples is possible through diverse statistics with the "Past version 1.75b" software (Hammer et al., 2001); most of these indices being explained in Harper (1999). Here, we calculated the number of taxa per sample (S), the dominance (D) that ranges from 0 (all taxa are equally present) to 1 (one taxon dominates the community completely), and the Margalef's richness index: $(S - 1)/ \ln(n)$, where n is the number of individuals counted in each sample.

Quantitative estimates of past sea-surface parameters

We used the Modern Analogue Technique (MAT) based on the statistical distance between fossil (paleoceanographic record) and current (modern database) assemblages (de Vernal et al., 2001; 2005; Guiot and de Vernal; 2007). The dinocyst transfer function used (Radi and de Vernal, 2008) is derived from a modern database comprising 67 dinocyst species and 1,492 stations from the North Atlantic, Arctic and North Pacific oceans and their adjacent seas, and is run under the

Biogeosciences Discuss., doi:10.5194/bg-2016-144, 2016
Manuscript under review for journal Biogeosciences
Published: 21 April 2016

239 "R version 2.7.0" software (R Development Core Team, 2008; http://www.r-project.org/). The
240 calculation of past hydrological parameters relies on a weighted average of the values obtained
241 for a maximum of 5 best modern analogues for fossil assemblages; the maximum weight being
242 given for the closest analogue (i.e. minimal statistical distance, or "Dmin). If "Dmin" reaches a
243 maximal threshold value, the "R" software will consider no analogue, leading then occasionally
244 to non analogue configurations. Here, we discuss Winter/Summer SST with prediction errors of
245 ±1.2°C/±1.6°C, respectively, Winter/Summer SSS, with prediction errors of ±2.1°C/±2.3°C,
246 respectively, as well as primary productivity reconstructions with prediction error of 57 $gC.m^{-2}$.
247

Biogeosciences Discuss., doi:10.5194/bg-2016-144, 2016
Manuscript under review for journal Biogeosciences
Published: 21 April 2016

248 **4. MAIN DINOCYST RESULTS ACROSS THE LAST 50 KY IN THE GULF OF CADIZ**

249 ***4.1. Dinocyst diversity, concentrations, and fluxes***

250 Dinocyst diversity is characterized by an average of 20 main species; 40 different species in total
251 being observed in the section. Considering the whole dinocyst assemblage, decreased total
252 diversity (Figure 4c) generally appears anti-correlated to increased dominance (Figure 4d); this
253 index being essentially explained by *Lingulodinium machaerophorum* percentages through time
254 (Figure 4e) that oscillate between 30 and 90%. *L. machaerophorum* is commonly considered as a
255 typical index species for stratified waters (Table 1; Zaragosi et al., 2001; Penaud et al., 2009;
256 Holzwarth et al., 2010), thus probably signing enhanced fluvial supplies. Since core MD99-2339
257 is located in the major flow path of the lower limb of the MOW, and in a position also
258 corresponding to the major limb of the MOW during the LGM (Rogerson et al., 2011), one can
259 speculate if the paleoceanographical record has been disturbed by MOW plume hydrodynamics
260 or advection by sedimentological processes (i.e. downslope transport). Large development of
261 monospecific species (when dominance is close to 1) will generally tend to reduce diversity and
262 conversely (dominance close to 0 reflecting an equidistribution of different species when the
263 diversity is maximum). Based on the obvious anti-correlation depicted in Figure 4 (diversity
264 *versus* dominance), we argue for an autochthonous assemblage where species, and especially *L.*
265 *machaerophorum*, reflect an *in situ* signal linked to changing sea-surface conditions.
266 Total dinocyst concentrations evidence an extremely large range of values (Figure 4f); higher
267 values (between 100,000 and 400,000 cysts/cm^3) being recorded between HS5 and HS3, with
268 maximal concentrations at 1,600-1,700 cm just after HS5 during GI 12 (Figure 4f). A general
269 trend of decreasing concentrations is then observed throughout the record with lower values
270 observed during the early to mid-Holocene (between 1,000 and 10,000 cysts/cm^3) and especially
271 at the very start of the Holocene (1,500 cysts/cm^3; at 150-200 cm), following the cold interval of
272 the Younger Dryas (YD) (Figure 4f). Also, minimum concentration values recorded during MIS

Biogeosciences Discuss., doi:10.5194/bg-2016-144, 2016
Manuscript under review for journal Biogeosciences
Published: 21 April 2016

3 are comparable to maximum values recorded during following MIS 2 and MIS 1. The general trend described above closely matches the one of sedimentation rates (Figure 4h) and thus also accounts for extremely high dinocyst fluxes to the seafloor during MIS 3 (Figure 4j), compared to the last deglaciation and the Holocene. Total dinocyst concentrations are mainly explained by *L. machaerophorum* alone (Figure 4h), showing the crucial role of this species regarding dinocyst export to the seafloor from the last glacial to present in this subtropical NE Atlantic area. While heterotrophics represent a minor component of total dinocyst concentrations all along the core (Figure 4g), it is interesting to note that both heterotrophic and *L. machaerophorum* concentrations/fluxes reveal the same decreasing trend along the record (Figure 4j).

4.2. Dinocyst species reflecting qualitatively main paleohydrological changes

Present-day ecologies of major species found in assemblages of MD99-2339 core are listed in Table 1 with their major past occurrences in the fossil record. The detailed examination of the qualitative thermic index "Warm/Cold" (W/C) (Table 1; Figure 5; cf. subchapter 3.2.2 of this paper), compared with the planktonic $\delta^{18}O$ curve (*G. bulloides*) of core MD99-2339 (Voelker et al., 2006), shows that millennial-scale climate variability related to the GS / GI cycles is clearly captured by our fossil record then confirming the robustness of reconstructed surface environments through dinocyst assemblages in the central Gulf of Cadiz.

Specific percentages, calculated relatively to the total dinocyst assemblages but also *versus* a total that excludes *L. machaerophorum*, reveal that trends with or without *L. machaerophorum* are similar (Figure 5). Peak occurrences are, however, better expressed when *L. machaerophorum* is omitted from the main palynological sum. Figure 5 furthermore includes the published data from core MD04-2805 CQ (Figure 1) over the last 28 ky (Penaud et al., 2010; dotted lines in Figure 5). Obvious correlation between surface conditions recorded off the NW Moroccan coast (Marret and Turon, 1994; Penaud et al., 2010) and in the central part of the Gulf of Cadiz may be due to

Biogeosciences Discuss., doi:10.5194/bg-2016-144, 2016
Manuscript under review for journal Biogeosciences
Published: 21 April 2016

same dynamics governing paleohydrological changes in this sector (Penaud et al., 2011a). Considering more specifically hetrotrophics, these are never dominant among studied assemblages (Figure 5). Heterotrophics are well known to be sensitive to oxic conditions (e.g. Combourieu-Nebout et al., 1998; Zonneveld et al., 1997b; Kodrans-Nsiah et al., 2008), and the fact that *Brigantedinium* percentages increased during GS (i.e. periods with relatively well-oxygenated bottom waters related to MOW dynamics) may argue for a negligible effect of oxidation processes on species-selective degradation after cyst deposition in our study site. Significant occurrences of some selected species (Table 1; Penaud et al., 2011a), and especially coastal heterotrophics (*S. quanta* and *S. nephroides*; Figure 5), will then indirectly reflect varying regimes of mesotrophic-oligotrophic conditions in the Gulf of Cadiz over the last 50 ky.

Biogeosciences Discuss., doi:10.5194/bg-2016-144, 2016
Manuscript under review for journal Biogeosciences
Published: 21 April 2016

5. UNDERLYING MECHANISMS BEHIND DINOCYST CHANGES AT ORBITAL AND SUB-ORBITAL TIMESCALES IN THE GULF OF CADIZ

Portuguese-Moroccan upwelling dynamics are of particular interest since planktonic populations are directly linked there to frontal areas and upwelled nutrient-enriched waters. At the Quaternary timescale, biodiversity increases have previously been observed during glacial periods, as a probable consequence of an enhanced functioning of upwelling cells (Abrantes, 1988, 1991; Targarona, 1997; Penaud et al., 2011a) and strong biodiversity modifications have been related to abrupt climate changes such as cold GS and especially HS (Lebreiro et al., 1997; Eynaud et al., 2000; Voelker et al., 2006; Penaud et al., 2011a, b) with a total re-structuration of the water column. Understanding mechanisms underlying the complex pattern of paleoproductivity changes at orbital as well as millennial timescales thus includes considering a wide range of external and internal forcing, i.e. varying conditions in terms of sea level, insolation, wind-stress, water-mass exchanges at the Gibraltar Strait, iceberg or fluvial discharges, and frontal upwelling cells; all of these being more or less inter-connected at different timescales.

5.1. Glacial fertilisation control on marine surface productivity

Annual productivity quantifications calculated from dinocyst transfer function (Figure 6), the qualitative ratio H/A, as well as dinocyst fluxes (total and heterotrophics), evidence higher productivities during MIS 3 and MIS 2, compared to the last deglaciation and the Holocene, with a sharp transition noted at 15 ka BP (Figure 6). Similar decreasing paleo-productivity at the end of the last glacial period was also previously discussed in the Gulf of Cadiz in a nearby core based on planktonic foraminifera-derived productivity quantifications (Wienberg et al., 2010). Glacial productivity rise is commonly attributed to a fertilisation effect caused by increasing aeolian dust supply to the ocean under stronger glacial winds (Moreno et al., 2002; Bout-Roumazeilles et al., 2007; Wienberg et al., 2010), combined with higher Mediterranean

Biogeosciences Discuss., doi:10.5194/bg-2016-144, 2016
Manuscript under review for journal Biogeosciences
Published: 21 April 2016

334 continental aridity (Combourieu-Nebout et al., 2002; Sanchez-Goni et al., 2002; Bar-Matthews et
335 al., 2003; Fletcher and Sanchez-Goni, 2008). Also, during MIS2, glacial productivity
336 reconstructed in the Gulf of Cadiz through dinocyst assemblages are the highest (around 500
337 GC/m² compared to present-day values of about 90 gC/m²; Figure 6). It was suggested to be
338 regionally due to upwelled nutrient-enriched waters linked to the occurrence of a comparable
339 hydrographic barrier to the modern Azores Front (Rogerson et al., 2004, 2010; Voelker et al.,
340 2009). This is also suggested in our record with enhanced *Brigantedinium* (Figure 7) and total
341 hetrotrophic percentages (H/A; Figure 6) between 26 and 15 ka BP (Penaud et al., 2011a).
342
343 ***5.2. Orbital control on paleo-river discharges and nutrient availability***
344 Furthermore, when considering *L. machaerophorum* percentages *versus* orbital parameters, a
345 very close relationship to the obliquity curve becomes obvious (Figure 7). Assuming this species
346 as a strong fluvial-sensitive cyst (Table 1), we may suggest enhanced precipitation in the southern
347 borderlands of the Mediterranean Basin with obliquity maxima, the latter accounting for
348 increasing northern summer insolation. Furthermore, generally higher percentages of *L.*
349 *machaerophorum* recorded between 50 and 35 ka BP coincide with extremely high total dinocyst
350 concentrations (fluxes), while generally higher percentages of *L. machaerophorum* recorded from
351 15 ka BP onwards coincide with extremely low total dinocyst concentrations (/fluxes) (Figure 7).
352 The Mediterranean Basin being subject to interference of northern and tropical latitudes, both
353 obliquity and precession signals may be considered. They indeed represent major influences for
354 the East African and West Indian summer monsoon systems (Tuenter et al., 2003) and can be
355 evidenced, for instance, in Mediterranean paleorecords (Lourens et al., 1996, 2001). Furthermore,
356 Tuenter et al. (2003) discussed the fact that the combination “obliquity maxima - precession
357 minima” (cf. MIS 1 in Figure 7) would have a weaker effect on the African monsoon, compared
358 to the combination “obliquity maxima - precession maxima” (cf. MIS 3 in Figure 7). This would

Biogeosciences Discuss., doi:10.5194/bg-2016-144, 2016
Manuscript under review for journal Biogeosciences
Published: 21 April 2016

359 be consistent, during MIS 1, with our recorded enhanced stratification related to lower
360 productivities (Figure 6), especially between 10 and 6 ka BP, and our recorded enhanced
361 stratification during periods of higher productivities across the last glacial (Figure 6).
362 Also, interestingly, similar high Gulf of Cadiz dinocyst concentrations (fluxes) and *L.*
363 *machaerophorum* percentages are recorded in the northern Bay of Biscay during the mid-
364 Holocene (Naughton et al., 2007; Ganne et al., in prep). We can assume that high nutrient
365 availability in the Gulf of Cadiz during the last glacial may has been similarly high to modern
366 nutrient availability in northern latitudes of the temperate NE Atlantic (Bay of Biscay). This
367 northward migration of paleo-productive centers is also similar to the migration of cold-water
368 corals, from the Gulf of Cadiz during the last glacial period to the Irish-Norwegian margins at
369 present (Freiwald et al., 2004; Dorschel et al., 2005; Rüggeberg et al., 2007; Eisele et al., 2008;
370 Frank et al., 2005, 2009; de Haas et al., 2009; Wienberg et al., 2009, 2010). We then suggest
371 maxima in dinocyst, and perhaps phytoplanktonic organisms in general, export during glacial
372 obliquity maxima in subtropical latitudes, when ice-sheets were still well developed in the
373 Northern Hemisphere, while interglacial obliquity maxima would preferentially stimulate
374 phytoplanktonic growth in northern latitudes of the North Atlantic. Marine surface productivity
375 has been tentatively modelled for the Indian Ocean with simulations coupling a biogeochemical
376 component for primary production, from 80 ka BP climate conditions to the preindustrial state
377 (Le Mézo et al., unpublished data, EGU2015). It evidences the crucial role of obliquity, i.e.
378 glacial-interglacial conditions responsible for changing oceanic circulation, as a main driver for
379 phytoplanktonic productivities.
380
381 ***5.3. MIS 3 and the atypical pattern of Greenland Interstadials GI 8 and GI 12***
382 *5.3.1. General overview of MIS 3 pattern on either side of the Strait of Gibraltar*
383 MIS 3 corresponds to a general stronger velocity of denser MOW export (Grain-size analysis;

Biogeosciences Discuss., doi:10.5194/bg-2016-144, 2016
Manuscript under review for journal Biogeosciences
Published: 21 April 2016

384 Figure 7). Over this period, dinocyst signals from both sides of the Strait of Gibraltar, i.e. signals
385 recorded from the Gulf of Cadiz (this study) and the Alboran Sea (MD95-2043 core; Penaud et
386 al., 2011b; Figure 1), have been compared so as to qualify Mediterranean/Atlantic surface
387 exchanges at times when MOW experienced strongest/weakest bottom current velocities (Figure
388 8).
389 A first look on dinocyst concentrations for selected individual species (Figure 8d,e,f) reveals
390 extremely close patterns from either sides of the Strait of Gibraltar, however, with different
391 magnitude of values, especially when considering *L. machaerophorum* concentrations that are 10
392 to 100 times higher in the Gulf of Cadiz compared to the Alboran Sea (Figure 8d). Total dinocyst
393 concentrations are also characterized by similar temporal fluctuations but different reconstructed
394 values; these marked value differences being only explained by *L. machaerophorum*
395 concentrations since other "autotrophic" species show generally comparable orders of
396 concentrations (Figure 8g).
397 It is interesting to note that even if individual species concentrations follow obvious identical
398 oscillations, they are not as clear when considering their relative abundances (Figure 8k, l, m). *L.*
399 *machaerophorum* percentages generally dominate whole cyst assemblages all over MIS 3 in the
400 Gulf of Cadiz, such as today (Rochon et al., 1999; Marret and Zonneveld, 2003; Zonneveld et al.,
401 2013; Table 1; Figure 8k). In the Alboran Sea, *N. labyrinthus* (cool-temperate, outer neritic)
402 percentages mirror *L. machaerophorum* (temperate, inner-neritic) ones in the Gulf of Cadiz
403 (Figure 8l); this species hardly making up 5% of the present-day assemblage in the area. When
404 these two species are summed, their percentages show obvious similar patterns both in terms of
405 values and timing of the different recorded peaks (Figure 8n). Combined "*N. labyrinthus-L.*
406 *machaerophorum*" percentages are not clearly related to GS or GI climate conditions, however
407 features can be distinguished: i) maximal values are recorded at the end of GI 8 and 12, but very
408 low values at the start of these specific interstadials, ii) they never occur during HS with

Biogeosciences Discuss., doi:10.5194/bg-2016-144, 2016
Manuscript under review for journal Biogeosciences
Published: 21 April 2016

409 significant percentages, and iii) they often characterize GS climate conditions with increasing
410 relative abundances (Figure 8n).
411
412 *5.3.2. Greenland Stadial (GS) and especially Heinrich Stadial (HS)*
413 During GS, and especially HS, dinocyst seasonal SST reconstructions from the Gulf of Cadiz
414 evidence a 2 to 5°C cooling, as a consequence of the southward shift of the Polar Front (e.g.
415 Eynaud et al., 2009). This is especially true for winter SST (Figure 6); dry and cold winter
416 conditions being also previously recorded in these latitudes (Sanchez-Goni et al., 2002;
417 Combourieu-Nebout et al., 2002; Moreno et al., 2002, 2005; Bout-Roumazeilles et al., 2007). *B.*
418 *tepikiense* combined with the polar foraminifera *N. pachyderma* s. attest, respectively, to enhance
419 seasonality (large offset between summer and winter temperatures as confirmed by dinocyst
420 transfer function; Figure 6) and important coolings in the interval 25-50 ka BP (Figure 6). "*N.*
421 *pachyderma* s. - *B. tepikiense"* thus evidence in both the Gulf of Cadiz and the Alboran Sea the
422 impact of subpolar water masses into these subtropical north-eastern Atlantic latitudes (Sanchez-
423 Goni et al., 2000; Pailler and Bard, 2002; Turon et al., 2003; de Abreu et al., 2003; Vautravers
424 and Shackleton, 2006; Eynaud et al., 2000, 2009; Salgueiro et al., 2010, 2014; Patton et al., 2011;
425 Penaud et al., 2011a,b), also accounting for direct and strong surface connections responsible for
426 similar planktonic species occurrences at both sides of the Strait (Figure 8). During HS, this
427 occurs in a context when bottom MOW experienced intermediate (and not the strongest)
428 velocities because of the strong advection of less saline waters at the surface in the Western
429 Mediterranean Basin (Cacho et al., 2000; Sierro et al., 2005; Voelker et al., 2006; Frigola et al.,
430 2008).
431 In the Gulf of Cadiz, during HS, increased annual productivity reconstructions (Figure 6)
432 together with increased heterotrophics (especially *Brigantedinium* spp; Figure 7), suggest
433 primary productivity increases related to frontal system reorganizations within the Gulf of Cadiz

Biogeosciences Discuss., doi:10.5194/bg-2016-144, 2016
Manuscript under review for journal Biogeosciences
Published: 21 April 2016

434 (Rogerson et al., 2004, 2010; Voelker et al., 2009). This front was also discussed over the last 28
435 ky BP by the strong decreasing gradient of *N. pachyderma* s. percentages obvious during HS
436 across a small N-S transect between southern Portugal and the sector Cadiz-Morocco (Penaud et
437 al., 2011a). This configuration is similar to the one previously discussed for the LGM interval
438 that recorded the highest productivities and *Brigantedinium* percentages in our Gulf of Cadiz
439 fossil record (Figures 6 and 7). Except for HS, other GS are not systematically marked by such
440 features. Also, it is interesting to note that productivity drops were noted during GS in the same
441 core with planktonic foraminiferal Cd/Ca values, thus suggesting low nutrient availability at that
442 time (Patton et al., 2011). Our frontal upwelling conditions explaining higher productivities
443 would thus be especially valid for HS climate extrema in the Gulf of Cadiz. In the northern North
444 Atlantic, biomass decline has conversely been linked to abrupt climate changes (Schmittner,
445 2005; Mariotti et al., 2012) during AMOC disruption linked with massive iceberg calving (e.g.
446 McManus et al., 2004; Gherardi et al., 2005).
447
448 *5.3.3. Greenland Interstadial (GI) and especially GI 8 and GI 12: typical bipartite structure*
449 In the Gulf of Cadiz, warmer surface conditions are generally recorded during GI, as deduced
450 from the W/C ratio (Figure 5) and seasonal SST reconstructions with values close to modern ones
451 (Figure 6). The synchronous occurrences of thermophilic species *S. mirabilis* on both sides of the
452 Gibraltar Strait (Figure 8c) also attest of general warmer surface conditions, at a time when
453 bottom MOW velocity is reduced.
454 However, GI 12 and 8, immediately following HS 5 and 4 respectively, are characterized by very
455 peculiar features, unique in all the record when considering other GIs. These intervals show
456 periods characterized by the longest and strongest expansions of mixed oak forest over MIS 3
457 (Alboran Sea; Fletcher and Sanchez Goni, 2008; Figure 7) and, from a unique hydrological point
458 of view, they can be described according to a bipartite structure in the Gulf of Cadiz (cf. “a” and

Biogeosciences Discuss., doi:10.5194/bg-2016-144, 2016
Manuscript under review for journal Biogeosciences
Published: 21 April 2016

459 "b"; Figures 7), also previously described for the Alboran Sea (Penaud et al., 2011b; cf. parts a
460 and b; Figures 7). While the first part ("a"; Figure 8) is characterized by increasing coastal
461 heterotrophics (Figure 8o) and thermophilic species (Figure 8c), paralleling higher polar air
462 temperatures (Figure 8j); the second part ("b", Figure 8) is characterized by the highest total
463 dinocyst concentrations (Figure 8h) and *L. machaerophorum* percentages (Figure 8k) ever
464 recorded over the last 50 ky. This second part is also characterized by a strong *S. mirabilis* drop
465 (Figure 8c), and the lowest winter SST (minus 10°C compared with today; Figure 6) and SSS
466 (around 30 psu reconstructed at that time; Figure 6). We therefore suggest a major atmospheric
467 reorganization occurring at 37 ka BP within GI 8, and at 45.5 ka BP within GI 12, also detected
468 in NGRIP with decreasing polar temperatures all along these long interstadials (Figure 8j).
469 Within both second phases ("b", Figure 8), synchronous high *L. machaerophorum* percentages
470 recorded from subtropical NE Atlantic (quasi monospecific in the Gulf of Cadiz) and Western
471 Mediterranean basins, attest to extremely high fluvial discharges and well-stratified conditions.
472 We therefore suggest an extreme southward shift of the winter westerlies belt, more pronounced
473 during each part "b" than during each part "a", that would also be responsible for huge advection
474 of freshwater, especially during the winter season, and therefore reduced SST and SSS. This
475 questions the feedbacks inherent to the atmospheric/oceanic reorganisations. Even if the precise
476 mechanism underlying this shift is still questioned and would deserve model simulations, our
477 results argue for a fast response of the ocean in this millennial / infra-millennial-timescale context
478 of rapid climate change.
479
480 ***5.4. Dinocyst specific pattern across MIS 1***
481 Interestingly, during MIS 1, decreased dinocyst fluxes and increased *Impagidinium* percentages
482 (Figure 7) are obviously related to the humidity pattern as recorded in Western (Fletcher and
483 Sanchez-Goni, 2008; Figure 7) and Eastern (Bar-Matthews et al., 2000, 2003; Figure 7)

Biogeosciences Discuss., doi:10.5194/bg-2016-144, 2016
Manuscript under review for journal Biogeosciences
Published: 21 April 2016

484 Mediterranean records. During the first half of the Bölling-Alleröd (BA), *Impagidinium* species
485 (especially *I. aculeatum*; Figure 5) strongly expand (Figure 7), arguing for the establishment of
486 full oceanic and warm conditions, that may suggest oligotrophic conditions in this area (cf.
487 dinocyst transfer function; Figure 6) progressively replacing glacial eutrophic to mesotrophic
488 ones (Behrenfeld et al., 2005; Wienberg et al., 2010). This shift is synchronous to widespread
489 rainfalls over the entire Mediterranean Sea (Toucanne et al., 2015). Increased vegetation cover at
490 that time (Fletcher and Sanchez-Goñi, 2008; Figure 7) and thus decreased river runoff onland
491 may have also induced decreased nutrient supplies to the ocean. It is interesting to note that, in
492 North Atlantic subtropical latitudes, each onset of warm conditions during climatic optima (i.e.
493 MIS 1, 5, 11 and 19) was associated with the expansion of *Impagidinium* species (Eynaud et al.,
494 2016). This group thus marked post-glacial conditions instead of hypsithermal ones when a
495 competition with other thermophilous taxa such as *S. mirabilis* is observed (Turon and Londeix,
496 1988; Londeix et al., 2007; Eynaud et al., 2000, 2016; Penaud et al., 2008). Noteworthy, and
497 similar to GI 8 and 12, the BA is not homogeneous and is marked by a bipartite structure (cf.
498 phases “a” and “b” in Figure 7). The final BA (“b”) is indeed marked by a drastic drop of
499 *Impagidinium* spp, a strong increase of *L. machaerophorum* percentages and high values of total
500 dinocyst concentrations (Figure 7). This may suggest slightly more productive conditions (cf.
501 Figure 6) that followed mean general Mediterranean aridity increases starting as soon as 14 ka BP
502 and continuing during the following cold event of the YD (Figures 6 and 7).
503 Then, at the Holocene onset, during the 9.5-6.5 ka BP interval, the proportion of clay cohesive
504 sediments (cf. grain-size<63 µm; Figure 7) observed in core MD99-2339 is the largest of the
505 record, then suggesting a strong reduction of MOW flow strength (Voelker et al., 2006), as also
506 evidenced in Western Mediterranean Sea contourites from the Corsica through (Toucanne et al.,
507 2012). This early Holocene interval is coeval with enhanced summer precipitation over the
508 northern borderlands of the Eastern Mediterranean (i.e. North African summer monsoon forcing;

Biogeosciences Discuss., doi:10.5194/bg-2016-144, 2016
Manuscript under review for journal Biogeosciences
Published: 21 April 2016

509 Rossignol-Strick, 1983; Rohling and Hilgen, 1991; Bar-Matthews et al., 2000, 2003; Figure 7)
510 and thus increasing summer/autumn fluvial discharges mainly from the Nile (deMenocal et al.,
511 2000; Gasse, 2000). This leads, in the Eastern Mediterranean Sea, to important water column
512 stratification, a cessation of the deep convection, an anoxic phase of bottom waters, high surface
513 productivity, and thus to the rich-organic sapropel 1 formation (e.g. Kallel et al., 1997; Mercone
514 et al., 2000). Also, the Western Mediterranean Basin was subject to enhanced rainfalls (Aritzegui
515 et al., 2000; Zanchetta et al., 2007; Magny et al., 2013), and this has been recently connected to
516 seasonal Mediterranean autumn/winter rainfalls sustaining high fluxes of nutrients and organic
517 matter to the seafloor (Toucanne et al., 2015). Conversely, in our study, the period between 9.5
518 and 6.5 ka BP is characterized by low quantified productivities (Figure 6), the lowest dinocyst
519 fluxes (Figure 6) and by the highest percentages of *Impagidinium* spp ever recorded over the last
520 50 ky BP (Figure 7). Full-oceanic oligotrophic conditions have prevailed in the central Gulf of
521 Cadiz, and this can be attributed to significantly lower amounts of Saharan dust inputs at that
522 time (Wienberg et al., 2010) in a context when Mediterranean forest strongly expanded (Fletcher
523 and Sanchez-Goni, 2008; Figure 7) preventing dust re-mobilization and run-off. Furthermore, at
524 the time of sapropel 1 formation (Toucanne et al., 2015), a displacement of the autumn/winter
525 storm track along the northern Mediterranean borderlands (i.e. atmospheric configuration
526 extremely close to a persistence of negative NAO conditions) could have been favourable to a
527 southward winter displacement of the Azores High reinforcing the Azores Current influence
528 towards the Gulf of Cadiz, and therefore also probably the advection of nutrient-poor subtropical
529 North Atlantic Central Water during winter. This would also be consistent with the occurrence of
530 thermophilous *Impagidinium* species, mainly encountered today in fully marine tropical
531 environments (Bouimetarhan et al., 2009). Also, in the Gulf of Cadiz, the Levantine Intermediate
532 Water (LIW) directly contribute to the upper MOW export during interglacials, while a
533 downslope shift of the denser MOW plume is noted during glacials/lowstands (Voelker et al.,

534 2006; Toucanne et al., 2012; Kaboth et al., 2015). We can then hypothesize that, during the
535 Holocene, the cessation of LIW formation in the Eastern Mediterranean may have impacted the
536 remobilization of sediments/nutrients through the lack of mixing at the subsurface between
537 surface and deep current across the Strait of Gibraltar (Gomez et al., 2000), also additionally
538 contributing to the decreased dinocyst fluxes recorded in the central Gulf of Cadiz (Figure 7).
539
540 **6. CONCLUSION**
541 New palynological investigations carried out in the central part of the Gulf of Cadiz over MIS 3
542 (25-50 ka BP) enable to consider dinocyst population shifts over the last 50 ky in the subtropical
543 north-eastern Atlantic Ocean; dinocyst studies in subtropical latitudes being much less frequent
544 than those performed in northern basins of the North Atlantic, though they deserve a crucial role
545 in the carbon pump at a global scale. We especially focus on the dinocyst species *L.*
546 *machaerophorum* that we interpret as a powerful tool to discuss surface hydrological changes
547 through time in the north-eastern Atlantic, and especially water column stratification under
548 varying regimes of paleo-precipitations, primarily forced by obliquity maxima at orbital
549 timescales. Dinocyst fluxes, and perhaps also dinoflagellate productive conditions, in the Gulf of
550 Cadiz were the highest during the last glacial (especially between GI8 and GI12), and a clear
551 imprint of millennial-scale abrupt climate changes was detected on paleohydrological changes all
552 over the investigated period. During the Holocene, precessional forcing is also suggested through
553 the probable impact of sapropel 1 formation in the Eastern Mediterranean on decreasing dinocyst
554 fluxes and perhaps also on dinoflagellate productivity in the Gulf of Cadiz. This study finally
555 provides important evidences of migrating paleoproductivity centres from the last glacial period
556 to the Holocene, and can be therefore also of crucial importance for our understanding of long-
557 term and abrupt climate changes in primary productivity regimes and organic matter export to the
558 seafloor.

Biogeosciences Discuss., doi:10.5194/bg-2016-144, 2016
Manuscript under review for journal Biogeosciences
Published: 21 April 2016

559 **7. ACKNOWLEDGMENTS**

560 Thanks to the French polar institute IPEV (*Institut Paul Emile Victor*), the captain and the crew
561 of the Marion Dufresne and the scientific team of the 1995 IMAGES cruise. We wish to thank M.
562 Castera, M. Georget and O. Ther for invaluable technical assistance at the laboratory. This study
563 was supported by the French CNRS and contributes to the 2013 INSU project : « ICE-BIO-RAM
564 : Impact des Changements Environnementaux sur la BIOdiversité marine lors des
565 Réchauffements Abrupts du cliMat » (http://www.insu.cnrs.fr/files/ao_2013_-
566 _eynaud_validee.pdf). This work was supported by the «Laboratoire d'Excellence» LabexMER
567 (ANR-10-LABX-19) and co-funded by a grant from the French government under the program
568 «Investissements d'Avenir». AV acknowledges her Investigador FCT (IF) Development Grant.

569

570

Biogeosciences Discuss., doi:10.5194/bg-2016-144, 2016
Manuscript under review for journal Biogeosciences
Published: 21 April 2016

8. REFERENCES

Abrantes, F., 1988. Diatom assemblages as upwelling indicators in surface sediments off Portugal. Marine Geology 85, 15-39.

Abrantes, F., 1991. Increased upwelling off Portugal during the last glaciation: diatom evidence. Mar. Micropaleontol. 17, 285-310.

Alvarez, M., Pérez, F.F. Shoosmith, D.R. Bryden. H.L. 2005. The unaccounted role of Mediterranean water in the draw–down of anthropogenic carbon. J. Geophys. Res. 110, C09S03, doi: 10.1029/2004JC002633.

Alves, M., de Verdière, A.C., 1999. Instability dynamics of a subtropical jet and applications to the Azores Front current system: Eddy driven mean flow, Journal of Physical Oceanography 29, 837-864.

Alves, M., Gaillard, F., Sparrow, M., Knoll, M., Giraud, S., 2002. Circulation patterns and transport of the Azores Front-current system. Deep-Sea Research II 49, 3 983-4 002.

Ambar, I., Serra, N., Brogueira, M.J., Cabecadas, G., Abrantes, F., Freitas, P., Goncalves, C., Gonzalez, N., 2002. Physical, chemical and sedimentological aspects of the Mediterranean outflow off Iberia. Deep-Sea Research II 49, 4163-4177.

Ambar, I., Howe, M. R., 1979. Observations of the Mediterranean outflow - I: Mixing in the Mediterranean outflow. Deep-Sea Res. 26, 535-554.

596 Aristegui, J., Alvarez-Salgado, X.A., Barton, E.D., Figueiras, F.G., Hernandez-Leon, S., Roy, C.,
597 Santos, A.M.P., 2005. Chapter 23: oceanography and fisheries of the Canary current/Iberian
598 region of the eastern North Atlantic (18a,E). In: Brink K.H. (ed.), Robinson A.R. (ed.) The sea :
599 the global coastal ocean : interdisciplinary regional studies and syntheses. Harvard: Harvard
600 University Press, 877-931.
601
602 Austin, W.E.N., Hibbert, F.D., 2012. Tracing time in the ocean: A brief review of chronological
603 constraints (60–8 kyr) on North Atlantic marine event-based stratigraphies, Quat. Sci. Rev., 36,
604 28-37.
605
606 Austin, W.E.N., Hibbert, F.D., Rasmussen, S.O., Peters, C., Abbott, P.M., Bryant, C.L., 2012.
607 The synchronization of palaeoclimatic events in the North Atlantic region during Greenland
608 Stadial 3 (ca 27.5 to 23.3 kyr b2k). Quat. Sci. Rev. 36, 154–163.
609
610 Bahr, A., Jiménez-Espejo, F.J., Kolasinac, N., Grunert, P., Hernández-Molina, F.J., Röhl, U.,
611 Voelker, A.H.L., Escutia, C., Stow, D.A.V., Hodell, D., Alvarez-Zarikian, C.A., 2014.
612 Deciphering bottom current velocity and paleoclimate signals from contourite deposits in the
613 Gulf of Cádiz during the last 140 kyr: an inorganic geochemical approach. Geochem. Geophys.
614 Geosyst. 15, 3145–3160.
615
616 Bahr, A., Kaboth, S., Jiménez-Espejo, F.J., Sierro, F.J., Voelker, A.H.L., Lourens, L., Röhl, U.,
617 Reichart, G.J., Escutia, C., Hernández-Molina, F.J., Pross, J., Friedrich, O., 2015. Persistent
618 monsoonal forcing of Mediterranean Outflow Water dynamics during the late Pleistocene.
619 Geology 43 (11), 951-954.
620

621 Bard, E., Rostek, R., Turon, J.L., Gendreau, S., 2000. Hydrological impact of Heinrich events in
622 the subtropical northeast Atlantic. Science 289, 1321-1324.
623
624 Bar-Matthews, M., Ayalon, A., Gilmour, M., Matthews, A., Hawkesworth, C.J., 2003. Sea-land
625 oxygen isotopic relationships from planktonic foraminifera and speleothems in the Eastern
626 Mediterranean region and their implication for paleorainfall during interglacial intervals.
627 Geochim. Cosmochim. Acta 67 (17), 3181-3199.
628
629 Bar-Matthews, M., Ayalon, A., Kaufman, A., 2000. Timing and hydrological conditions of
630 Sapropel events in the Eastern Mediterranean, as evident from speleothems, Soreq cave. Isr.
631 Chem. Geol. 169 (1-2), 145-156.
632
633 Barker, S., et al., 2009. Interhemispheric Atlantic seesaw response during the last deglaciation.
634 Nature 457 (7233), 1097-1102.
635
636 Behrenfeld, M.J., Boss, E., Siegel, D.A., Shea, D.M., 2005. Carbon-based ocean productivity and
637 phytoplankton physiology from space. Glob. Biogeochem. Cycles 19, GB1006.
638 doi:10.1029/2004GB002299.
639
640 Berger, A., Loutre, M.F., 1991. Insolation values for the climate of the last 10 million years.
641 Quaternary Science Reviews 10 (4), 297-317.
642
643 Biebow, N., 1996. Dinoflagellatenzysten als Indikatoren der spätund postglazialen Entwicklung
644 des Auftriebsgeschehens vor Peru. Geomar Report 57, 100 pp.
645

646 Bouimetarhan, I., Marret, F., Dupont, L., Zonneveld, K., 2009. Dinoflagellate cyst distribution in
647 marine surface sediments off West Africa (6-17°N) in relation to sea-surface conditions,
648 freshwater input and seasonal coastal upwelling. Marine Micropaleontology 71, 113-130.
649
650 Bout-Roumazeilles, V., Combourieu Nebout, N., Peyron, O., Cortijo, E., Landais, A., Masson-
651 Delmotte, V., 2007. Connection between South Mediterranean climate and North African
652 atmospheric circulation during the last 50,000 yr BP North Atlantic cold events. Quaternary
653 Science Reviews 26 (25-28), 3197-3215.
654
655 Caballero, I., Morris, E.P., Prieto, L., Navarro, G., 2014. The influence of the Guadalquivir River
656 on the spatio-temporal variability of suspended solids and chlorophyll in the Eastern Gulf of
657 Cadiz. Medit. Mar. Sci. 15 (4), 721-738.
658
659 Cacho, I., Grimalt, J.O., Sierro, F.J., Shackleton, N.J., Canals, M., 2000. Evidence for enhanced
660 Mediterranean thermohaline circulation during rapid climatic coolings. Earth and Planetary
661 Science Letters 183(3-4), 417-429.
662
663 Combourieu-Nebout, N., Paterne, M., Turon, J.L., Siani, G., 1998. A high resolution record of
664 the last deglaciation in the central Mediterranean Sea : palaeovegetation and palaeohydrological
665 evolution. Quaternary Science Reviews 17, 303-317.
666
667 Combourieu Nebout, N., Londeix, L., Baudin, F., Turon, J.L., von Grafenstein, R., Zahn, R.,
668 1999. Quaternary marine and continental paleoenvironments in the western Mediterranean (site
669 976, Alboran sea): Palynological evidence. Proceedings of the Ocean Drilling Program, Scientific
670 results 161, 457-468.

671

672 Combourieu-Nebout, N., Turon, J.L., Zahn, R., Capotondi, L., Londeix, L., Pahnke, K., 2002.
673 Enhanced aridity and atmospheric high-pressure stability over the western Mediterranean during
674 the North Atlantic cold events of the past 50 k.y. Geology 30, 863-866.

675

676 Dale, B., 1996. Dinoflagellate cyst ecology: modeling and geological applications. In: J.
677 Jansonius and D.C. McGregor (Editors), Palynology: principles and applications, Vol. 3. AASP
678 Foundation, Salt Lake City, 1 249-1 275.

679

680 Dale, B., Fjellså, A., 1994. Dinoflagellate cysts as paleoproductivity indicators: state of the art,
681 potential and limits. In: Zahn, R., Pedersen, T., Kaminiski, M., Labeyrie, L. (Eds.), Carbon
682 Cycling in the Glacial Ocean: Constrains on the Ocean. Role in Global Change. Springer-Verlag,
683 Berlin, 521-537.

684

685 Dale, B., Thorsen, T.A., Fjellså, A., 1999. Dinoflagellate cysts as indicator of cultural
686 eutrophication in the Oslofjord, Norway. Estuarine, Coastal and Shelf Science 48, 371-382.

687

688 Daniau, A.L., Sánchez-Goñi, M.F., Beaufort, L., Laggoun-Défarge, F., Loutre, M.F., Duprat, J.,
689 2007. Dansgaard-Oeschger climatic variability revealed by fire emissions in south-western Iberia.
690 Quat. Sci. Rev. 26, 1369-1383.

691

692 Dansgaard, W., Johnsen, S.J., Clausen, H.B., Dahl-Jensen, D., Gundestrup, N.S., Hammer, C.U.,
693 Hvidberg, C.S., Steffenson, J.P., Sveinbjörnsdottir, A.E., Jouzel, J., Bond, G., 1993. Evidence for
694 general instability of past climate from a 250-kyr ice-core record. Nature 364, 218-220.

695

696 de Abreu, L., Shackleton, N.J., Schönfeld, J., Hall, M., Chapman, M., 2003. Millennial-scale
697 oceanic climate variability off the western Iberian margin during the last two glacial periods.
698 Marine Geology 196, 1-20.
699
700 de Haas, H., Mienis, F., Frank, N., Richter, T.O., Steinbacher, R., de Stigter, H., van der Land,
701 C., van Weering, T.C.E., 2009. Morphology and sedimentology of (clustered) cold-water coral
702 mounds at the south Rockall Trough margins, NE Atlantic Ocean. Facies 55, 1-26.
703
704 de Leeuw, J.W., Versteegh, G.J.M., van Bergen, P.F., 2006. Biomacromolecules of algae and
705 plants and their fossil analogues. Plant Ecology 182, 209-233.
706
707 de Menocal, P., Ortiz, J., Guilderson, T., Adkins, J., Sarnthein, M., Baker, L., Yarusinsky, M.,
708 2000. Abrupt onset and termination of the African Humid Period: rapid climate responses to
709 gradual insolation forcing. Quaternary Science Reviews 19, 347-361.
710
711 de Vernal, A., Turon, J.L., Guiot, J., 1994. Dinoflagellate cyst distribution in high-latitude marine
712 environments and quantitative reconstruction of sea-surface salinity, temperature, and
713 seasonality. Canadian Journal of Earth Sciences 31, 48-62.
714
715 de Vernal, A., Henry, M., Bilodeau, G., 1999. Technique de préparation et d'analyse en
716 micropaléontologie. Les Cahiers du GEOTOP vol. 3, Université du Québec à Montréal,
717 Montréal, Canada.
718
719 de Vernal, A., Henry, M., Matthiessen, J., Mudie, P.J., Rochon, A., Boessenkool, K.P., Eynaud,
720 F., Grøsfjeld, K., Guiot, J., Hamel, D., Harland, R., Head, M.J., Kunz-Pirrung, M., Levac, E.,

721 Loucheur, V., Peyron, O., Pospelova, V., Radi, T., Turon, J.L., Voronina, E., 2001.
722 Dinoflagellate cyst assemblages as tracers of sea-surface conditions in the Northern North
723 Atlantic, Arctic and sub-Arctic seas: The new 'n = 677' data base and its application for
724 quantitative palaeoceanographic reconstruction. Journal of Quaternary Sciences 16, 681-698.
725
726 de Vernal, A., Eynaud, F., Henry, M., Hillaire-Marcel, C., Londeix, L., Mangin, S., Matthiessen,
727 J., Marret, F., Radi, T., Rochon, A., Solignac, S., Turon, J.L., 2005. Reconstruction of sea-surface
728 conditions at middle to high latitudes of the Northern Hemisphere during the last glacial
729 maximum (LGM) based on dinoflagellate cyst assemblages. Quat. Sci. Rev. 24, 897-924.
730
731 de Vernal, A., Marret, F., 2007. Organic-walled dinoflagellates : tracers of sea-surface
732 conditions, In Hillaire-Marcel and de Vernal (eds.) Proxies in Late Cenozoic Paleoceanography,
733 Elsevier, 371-408.
734
735 Devillers, R., de Vernal, A., 2000. Distribution of dinoflagellate cysts in surface sediments of the
736 northern North Atlantic in relation to nutrient content and productivity in surface waters. Marine
737 Geology 166, 103-124.
738
739 Dodge, J.D., Harland, R., 1991. The distribution of planktonic dinoflagellates and their cysts in
740 the eastern and north-eastern Atlantic Ocean. New Phytol. 118, 593-603.
741
742 Dorschel, B., Hebbeln, D., Rüggeberg, A., Dullo, W.C., 2005. Growth and erosion of a cold-
743 water coral covered carbonate mound in the Northeast Atlantic during the Late Pleistocene and
744 Holocene. Earth Planet. Sci. Lett. 233, 33-44.
745

746 Eisele, M., Hebbeln, D., Wienberg, C., 2008. Growth history of a cold-water coral covered
747 carbonate mound – Galway Mound, Porcupine Seabight. NE-Atlantic Mar. Geol. 253, 160-169.
748
749 Ellegaard, M., 2000. Variations in dinoflagellate cyst morphology under conditions of changing
750 salinity during the last 2000 years in the Limfjord, Denmark. Rev. Palaeobot. Palynol. 109, 65-
751 81.
752
753 Eynaud, F., 1999. Kystes de Dinoflagellés et Evolution paléoclimatique et paléohydrologique de
754 l'Atlantique Nord au cours du Dernier Cycle Climatique du Quaternaire. PhD, Bordeaux 1 Univ.,
755 291 pp.
756
757 Eynaud, F., Turon, J.L., Sánchez-Goñi, M.F., Gendreau, S., 2000. Dinoflagellate cyst evidence of
758 “Heinrich-like events” off Portugal during the marine isotopic stage 5. Mar. Micropal. 40, 9-21.
759
760 Eynaud, F., Turon, J.L., Duprat, J., 2004. Comparison of the Holocene and Eemian
761 palaeoenvironments in the South-Icelandic basin: dinoflagellate cysts as proxies for the North
762 Atlantic surface circulation. Review of Paleobotany and Palynology 128, 55-79.
763
764 Eynaud, F., de Abreu, L., Voelker, A., Schönfeld, J., Salgueiro, E., Turon, J.L., Penaud, A.,
765 Toucanne, S., Naughton, F., Sánchez-Goñi, M.F., Malaizé, B., Cacho, I., 2009. Position of the
766 Polar Front along the western Iberian margin during key cold episodes of the last 45 ka.
767 Geochem. Geophys. Geosyst. 10, Q07U05, doi:10.1029/2009GC002398.
768
769 Eynaud, F., Londeix L., Penaud A., Sanchez-Goni M.F., Oliveira D., Desprat S., Turon J.L.,
770 2016. Dinoflagellate cyst population evolution throughout past interglacials: key features along

771 the Iberian margin and insights from the new IODP Site U1385 (Exp 339). Global and Planetary
772 Change 136, 52-64.
773
774 Falkowski, P.G., Raven, J.A. 1997. Aquatic Photosynthesis. Blackwell Science, London, 375 pp.
775
776 Fasham, M.J.R., Platt, T., Irwin, B., Jones, K., 1985. Factors affecting the spatial pattern of the
777 Deep Chrolophyll Maximum in the region of the Azores Front, In: Crease, J., Gould, W.J.,
778 Saunders, P.M. (Eds.), Essays On Oceanography: A Tribute to John Swallow. Progress in
779 Oceanography 14, Pergamon, Oxford, 129-166.
780
781 Fensome, R.A., MacRae, R.A., Williams, G.L., 2008. DINOFLAJ2, Version1. American
782 Association of Stratigraphic Palynologists (DataSeries no. 1). Available at:
783 dinoflaj.smu.ca/wiki/Main_Page.
784
785 Fensome, R.A., Williams, G.L., 2004. The Lentin and Williams index of fossil dinoflagellates,
786 2004 edition. AASP Foundation Contributions Series 42, 909 pp.
787
788 Fiúza, A.F.G., Hamann, M., Ambar, I., Del Rio, G.D., González, N., Cabanas, J.M., 1998. Water
789 masses and their circulation off western Iberia during May 1993. Deep Sea Res. I 45, 1127-1160.
790
791 Flecha, S., Perez, F.F., Navarro, G., Ruiz, J., Olive, I., Rodriguez-Galvez, S., Costas, E.,
792 Huertas, I. E., 2012. Anthropogenic carbon inventory in the Gulf of Cadiz. J. Mar. Syst. 92, 67-
793 75.
794

795 Fletcher, W.J., Sánchez-Goñi M.F., 2008. Orbital- and sub-orbital scale climate impacts on
796 vegetation of the western Mediterranean basin over the last 48,000 yr. Quat. Res. 70, 451-464.
797
798 Frank, N., Lutringer, A., Paterne, M., Blamart, D., Henriet, J.-P., van Rooij, D., van Weering,
799 T.C.E., 2005. Deep-water corals of the northeastern Atlantic margin: carbonate mound evolution
800 and upper intermediate water ventilation during the Holocene. In: Freiwald, A., Roberts, J.M.
801 (Eds.), Cold-water Corals and Ecosystems. Springer, Heidelberg, pp. 113-133.
802
803 Frank, N., Ricard, E., Lutringer-Paque, A., van der Land, C., Colin, C., Blamart, D., Foubert, A.,
804 Van Rooij, D., Henriet, J.-P., de Haas, H., van Weering, T.C.E., 2009. The Holocene occurrence
805 of cold-water corals in the NE Atlantic: implications for coral carbonate mound evolution. Mar.
806 Geol. 266, 129-142.
807
808 Freiwald, A., Fosså, J.H., Grehan, A., Koslow, T., Roberts, J.M., 2004. Cold-water Coral Reefs.
809 UNEP-WCMC, Biodiversity Series 22, Cambridge, UK, pp. 84.
810
811 Frigola, J., Moreno, A., Cacho, I., Canals, M., Sierro, F.J., Flores, J.A., Grimalt, J.O., 2008.
812 Evidence of abrupt changes in Western Mediterranean Deep Water circulation during the last 50
813 kyr: A high-resolution marine record from the Balearic Sea. Quaternary International 181 (1), 88-
814 104.
815
816 Ganne, A., Penaud, A., Toucanne, S., Nizou, J., Hardy, W., Naughton, F., Eynaud, F., Bourillet,
817 J-F., in prep. Holocene rapid climate changes in the Bay of Biscay (NW France) as evidenced by
818 a crossed land-sea palynological approach over the last 9000 years.
819

820 Gherardi, J.M., Labeyrie, L., McManus, J.F., Francois, R., Skinner, L.C., Cortijo, E., 2005.
821 Evidence from the northeastern Atlantic basin for variability in the rate of the meridional
822 overturning circulation through the last deglaciation. Earth and Planetary Science Letters 240,
823 710-723.
824
825 Gómez, F., González, N., Echevarría, F., García, C.M., 2000. Distribution and Fluxes of
826 Dissolved Nutrients in the Strait of Gibraltar and its Relationships to Microphytoplankton
827 Biomass. Estuarine, Coastal and Shelf Science 51 (4), 439-449.
828
829 Gould, W.J. 1985. Physical oceanography of the Azores Front, in: J. Crease, W.J. Gould, P.M.
830 Saunders (Eds.), Essays in oceanography: A Tribute to John Swallow, Progress in Oceanography,
831 Pergamon, Oxford, 1985, pp. 167-190.
832
833 Grootes, P.M., Stuiver, M., White, J.W.C., Johnsen, S., Jouzel, J., 1993. Comparison of oxygen
834 isotope records from the GISP2 and GRIP Greenland ice cores. Nature 366, 552-554.
835
836 Grootes, P.M., Stuiver, M., 1997. Oxygen 18/16 variability in Greenland snow and ice with 103
837 to 105-year time resolution. Journal of Geophysical Research 102, 26,455-26,470.
838
839 Habgood, E.L., Kenyon, N.H., Masson, D.G., Akhmetzhanov, A., Weaver, P.P.E., Gardner, J.,
840 Mulder, T., 2003. Deep-water sediment wave fields, bottom current sand channels and gravity
841 flow channellobe systems: Gulf of Cadiz, NE Atlantic. Sedimentology 50, 483-510.
842

843 Hammer, Ø., Harper, D.A.T., Ryan, P.D., 2001. Past: Paleontological Statistics Software Package
844 for Education and Data Analysis. Palaeontologia Electronica, vol. 4, issue 1, art. 4: 9pp., 178kb.
845 http://palaeo-electronica.org/2001_1/past/issue1_01.htm.
846
847 Harland, R., 1983. Distribution maps of Recent dinoflagellate cysts in bottom sediments from the
848 North Atlantic Ocean and adjacent seas. Paleontology 26 (2), 321-387.
849
850 Harper, D.A.T. (ed.). 1999. Numerical Palaeobiology. John Wiley & Sons, Chichester.
851
852 Haynes, R., Barton, E.D., Pilling, I., 1993. Development, persistence, and variability of
853 upwelling filaments off the Atlantic coast of the Iberian Peninsula. J. Geophys. Res. 98 (C12),
854 22,681-22,692.
855
856 Head, M.J., 1996. Modern dinoflagellate cysts and their biological affinities. In "Palynology:
857 principles and Applications. Chapter 30." (Jansonius, J., and McGregor, D.C., editors), AASP
858 Foundation, 1,197-1,248.
859
860 Hernández-Molina, F.J., Stow, D.A.V., Alvarez-Zarikian, C.A., Acton, G., Bahr, A., Balestra, B.,
861 Ducassou, E., Flood, R., Flores, J.-A., Furota, S., Grunert, P., Hodell, D., Jimenez-Espejo, F.,
862 Kim, J.K., Krissek, L., Kuroda, J., Li, B., Llave, E., Lofi, J., Lourens, L., Miller, M., Nanayama,
863 F., Nishida, N., Richter, C., Roque, C., Pereira, H., Sanchez Goñi, M.F., Sierro, F.J., Singh, A.D.,
864 Sloss, C., Takashimizu, Y., Tzanova, A., Voelker, A., Williams, T., Xuan, C., 2014. Onset of
865 Mediterranean Outflow into the North Atlantic. Science 344, 1244-1250.
866

867 Holzwarth, U., Meggers, H., Esper, O., Kuhlmann, H., Freudenthal, T., Hensen, C., Zonneveld,
868 K.A.F., 2010. NW African climate variations during the last 47,000 years: Evidence from
869 organic-walled dinoflagellate cysts. Palaeogeography, Palaeoclimatology, Palaeoecology 291 (3-
870 4), 443-455.
871
872 Hsu, C.P.F., Wallace, J.M., 1976. The global distribution in annual and semiannual cycles in
873 precipitation. Monthly Weather Review 104 (9), 1093-1101.
874
875 Huertas, I.E., Navarro, G., Rodriguez-Galvez, S., Lubian, L.M., 2006. Temporal patterns of
876 carbon dioxide in relation to hydrological conditions and primary production in the northeastern
877 shelf of the Gulf of Cadiz (SW Spain). Deep-Sea Research II 53, 1,344-1,362.
878
879 Huertas, I. E., Rios, A.F., Garcia-Lafuente, J., Makaoui, A., Rodriguez-Galvez, S., Sanchez-
880 Roman, A., Orbi, A., Ruiz, J., Perez, F.F., 2009. Anthropogenic and natural CO2 exchange
881 through the Strait of Gibraltar. Biogeosciences 6, 647-662.
882
883 Ivanovic, R.F., Valdes, P.J., Flecker, R., Gregoire, L.J., Gutjahr, M., 2013. The parameterisation
884 of Mediterranean-Atlantic water exchange in the Hadley Centre model HadCM3, and its effect on
885 modelled North Atlantic climate. Ocean Modelling 62, 11-16.
886
887 Kaboth, S., Bahr, A., Reichart, G.J., Jacobs, B., Lourens, L.J., 2015. New insights into upper
888 MOW variability over the last 150 kyr from IODP 339 site U1386 in the Gulf of Cadiz. Marine
889 Geology, doi: 10.1016/j.margeo.2015.08.014.
890

891 Kallel, N., Paterne, M., Duplessy, J. C., Vergnaud-Grazzini, C., Pujol, C., Labeyrie, L., Arnold,
892 M., Fontugne, M., Pierre, C., 1997. Enhanced rainfall in the Mediterranean region during the last
893 sapropel event. Oceanologica Acta 20, 697-712.
894
895 Kodrans-Nsiah, M., de Lange, G.J., Zonneveld, K.A.F., 2008. A natural exposure experiment on
896 short-term species-selective aerobic degradation of dinoflagellate cysts. Review of Palaeobotany
897 and Palynology 152 (1-2), 32-39.
898
899 Labeyrie, L., Jansen, E., Cortijo, 2003. Les rapports de campagnes à la mer. MD 114/IMAGES V
900 OCE/2003/02. Brest, Institut Polaire Francais-Paul Emile Victor, 850 pp.
901
902 Lebreiro, S.M., Moreno, J.C., Abrantes, F.F., Pflaumann, U., 1997. Productivity and
903 paleoceanographic implications on the Tore Seamount (Iberian Margin) during the last 225 kyr:
904 Foraminiferal evidence. Paleoceanography 12 (5), 718-727.
905
906 Le Mézo, P., Kageyama, M., Bopp, L., Beaufort, L., 2015. Mechanisms behind primary
907 production distribution during the last glacial-interglacial cycle. Geophysical Research Abstracts
908 Vol. 17, EGU2015-880.
909
910 Lewis, J., Dodge, J.D., Powell, A.J., 1990. Quaternary dinoflagellate cysts from the upwelling
911 system off shore Peru, Hole 686B, ODP leg 112. Proc. ODP Sci. Results 112, 323-327.
912
913 Londeix, L., Benzakour, M., Suc, J.-P., Turon, J.L., 2007. Messinian palaeoenvironments and
914 hydrology in Sicily (Italy): The dinoflagellate cyst record. Geobios 40, 233-250.
915

916 Lourens, L.J., Antonarakou, A., Hilgen, F.J., Van Hoof, A.A.M., Vergnaud-Grazzini, C.,
917 Zachariasse, W.J., 1996. Evaluation of the Plio-Pleistocene astronomical timescale.
918 Paleoceanography 11 (4), 391-413.
919
920 Lourens, L.J., Wehausen, R., Brumsack, H.J., 2001. Geological constraints on tidal dissipation
921 and dynamical ellipticity of the Earth over the past three million years. Nature 409, 1029-1033.
922
923 Magny, M., et al., 2013. Northesouth palaeohydrological contrasts in the central Mediterranean
924 during the Holocene: tentative synthesis and working hypotheses. Clim. Past 9, 2043-2071.
925
926 Mariotti, V., Bopp, L., Tagliabue, A., Kageyama, M, Swingedouw, D., 2012. Marine productivity
927 response to Heinrich events: a model-data comparison. Clim. Past Discuss. 8, 557-594.
928
929 Marret, F., 1994. Distribution of dinoflagellate cysts in recent marine sediments from the east
930 Equatorial Atlantic (Gulf of Guinea). Review of Palaeobotany and Palynology 84, 1-22.
931
932 Marret, F., Turon, J.L., 1994. Paleohydrology and paleoclimatology off Northwest Africa during
933 the last glacial-interglacial transition and the Holocene: Palynological evidences. Marine Geology
934 118, 107-117.
935
936 Marret, F., Zonneveld, K.A.F., 2003. Atlas of modern organic-walled dinoflagellate cyst
937 distribution. Review of Palaeobotany and Palynology 125, 1-200.
938

939 McManus, J.F., Keigwin, L., Francois, R., Drown-Leger, S., Gherardi, J.M., 2004. Collapse and
940 rapid resumption of Atlantic meridional circulation linked to deglacial climate changes. Nature
941 428, 834-837.
942
943 McMinn, A., 1991. Recent dinoflagellate cysts from estuaries on the central coast of New South
944 Wales, Australia. Micropaleontology 37, 269-287.
945
946 Mercone, D., Thomson, J. Croudace, I.W. Siani, G. Paterne, M. Troelstra, S., 2000. Duration of
947 S1, the most recent sapropel in the eastern Mediterranean Sea, as indicated by accelerator mass
948 spectrometry radiocarbon and geochemical evidence. Paleoceanography 15, 336-347.
949
950 Mertens, K.N., Verhoeven, K., Verleye, T., Louwye, S., Amorim, A., Ribeiro, S., Deaf, A.S.,
951 Harding, I. C., De Schepper, S., Gonzalez, C., Kodrans-Nsiah, M., De Vernal, A., Henry, M.,
952 Radi, T., Dybkjaer, K., Poulsen, N.E., Feist-Burkhardt, S., Chitolie, J., Heilmann-Clausen, C.,
953 Londeix, L., Turon, J.L., Marret, F., Matthiessen, J., McCarthy, F.M.G., Prasad, V., Pospelova,
954 V., Kyffin Hughes, J.E., Riding, J.B., Rochon, A., Sangiorgi, F., Welters, N., Sinclair, N., Thun,
955 C., Soliman, A., Van Nieuwenhove, N., Vink, A., Young, M., 2009. Determining the absolute
956 abundance of dinoflagellate cysts in recent marine sediments: The Lycopodium marker-grain
957 method put to the test. Review of Palaeobotany and Palynology 157, 238-252.
958
959 Mertens, K. , Ribeiro, S., Bouimetarhan, I., Caner, H., Combourieu-Nebout, N., Dale, B., de
960 Vernal, A., Ellegaard, M., Filipova, M., Godhe, A., Grøsfjeld, K., Holzwarth, U., Kotthoff, U.,
961 Leroy, S., Londeix, L., Marret, F., Matsuoka, K., Mudie, P., Naudts, L., Peña-manjarrez, J.,
962 Persson, A., Popescu, S., Sangiorgi, F., van der Meer, M., Vink, A., Zonneveld, K., Vercauteren,
963 D., Vlassenbroeck, J., and Louwye, S. 2009b. Process length variation in cysts of a

964 dinoflagellate, Lingulodinium machaero¬phorum, in surface sediments investigating its potential
965 as salinity proxy. Marine Micropaleontology 70 (1-2), 54-69.
966
967 Moreno, A., Cacho, I., Canals, M., Prins, M.A., Sánchez-Goñi, M.F., Grimalt, J.O., Weltje, G.J.,
968 2002. Saharan dust transport and high-latitude glacial climatic variability: The Alboran Sea
969 record. Quaternary Research 58 (3), 318-328.
970
971 Moreno, A., Cacho, I., Canals, M., Grimalt, J.O., Sánchez-Goñi, M.F., Shackleton, N.J., Sierro,
972 F.J., 2005. Links between marine and atmospheric processes oscillating on a millennial time-
973 scale. A multiproxy study of the last 50,000 yr from the Alboran Sea (Western Mediterranean
974 Sea). Quaternary Science Reviews 24, 1623-1636.
975
976 Morzadec-Kerfourn, M.-T., Barros, A.M.A., Barros, A.B., 1990. Microfossiles a' paroi organique
977 et substances organiques des se¤diments holoce'nes de la lagune de Guarapina (Rio de Janeiro,
978 Brésil). Bull. Centres Rech. Explor.-Prod. Elf-Aquitaine 14, 575-582.
979
980 Naughton, F., Bourillet, J.F., Sánchez-Goni, M.F., Turon, J.L., Jouanneau, J.M., 2007. Long-term
981 and millennial-scale climate variability in northwestern France during the last 8850 years. The
982 Holocene 17 (7), 939-953.
983
984 Navarro, G., Ruiz, J., 2006. Spatial and temporal variability of phytoplankton in the Gulf of
985 Cadiz through remote sensing images. Deep-Sea Res. II 53, 1,241-1,260.
986
987 Nehring, S., 1994. Spatial distribution of dinoflagellate resting cysts in recent sediments of Kiel
988 Bight, Germany. Ophelia 39, 137-158.

989

990 Pailler, D., Bard, E., 2002. High frequency palaeoceanographic changes during the past 140 000
991 yr recorded by the organic matter in sediments of the Iberian Margin. Palaeogeography,
992 Palaeoclimatology, Palaeoecology 181 (4), 431-452.

993

994 Patton, G.M., Martin, P.A., Voelker, A., Salgueiro, E., 2011. Multiproxy comparison of
995 oceanographic temperature during Heinrich Events in the eastern subtropical Atlantic. Earth and
996 Planetary Science Letters 310 (1-2), 45-58.

997

998 Peliz, A., Dubert, J., Santos, A., Oliveira, P., Le Cann, B., 2005. Winter upper ocean circulation
999 in the Western Iberian Basin-Fronts, eddies and poleward flows: An overview. Deep Sea Res. I
1000 52, 621-646.

1001

1002 Peliz, A., Marchesiello, P., Santos, A.M.P., Dubert, J., Teles-Machado, A., Marta-Almeida, M.,
1003 Le Cann, B., 2009. Surface circulation in the Gulf of Cadiz: 2. Inflow-outflow coupling
1004 and the Gulf of Cadiz Slope Current. J. Geophys. Res. 114, C03011. http://dx.doi.org/
1005 10.1029/2008JC004771 16 pages.

1006

1007 Penaud, A., Eynaud, F., Turon, J.L., Zaragosi, S., Marret, F., Bourillet, J.F., 2008. Interglacial
1008 variability (MIS 5 and MIS 7) and dinoflagellate cyst assemblages in the Bay of Biscay (North
1009 Atlantic). Marine Micropaleontology 68, 136-155.

1010

1011 Penaud, A., Eynaud, F., Turon, J.L., Zaragosi, S., Malaizé, B., Toucanne, S., Bourillet, J.F., 2009.
1012 What forced the collapse of European ice sheets during the last two glacial periods (150 ka B.P.

and 18 ka cal B.P.)? Palynological evidence. Palaeogeography, Palaeoclimatology, Palaeoecology 281, 66-78.

Penaud, A., Eynaud, F., Turon, J.L., Blamart, D., Rossignol, L., Marret, F., Lopez-Martinez, C., Grimalt, J.O., Malaizé, B., Charlier, K., 2010. Contrasting Heinrich Events 1, 2, and LGM conditions off Morocco: Paleoceanographical evidences of warmer LGM and colder HE 1. Quaternary Science Reviews 29 (15-16), 1,923-1,939.

Penaud, A., Eynaud, F., Voelker, A., Kageyama, M., Marret, F., Turon, J.L., Blamart, D., Mulder, T., Rossignol, L., 2011. Assessment of sea surface temperature changes in the Gulf of Cadiz during the last 30 ka: implications for glacial changes in the regional hydrography. Biogeosciences 8, 2,295-2,316.

Penaud, A., Eynaud, F., Malaizé, B., Sanchez-Goñi, M., Turon, J.L., Rossignol, L., 2011b. Contrasting sea-surface responses between western Mediterranean Sea and eastern subtropical latitudes of the North Atlantic during the abrupt climatic events of MIS 3. Marine Micropaleontology 80 (1-2), 1-17.

Persson, A., Godhe, A., Karlson, B., 2000. Dinoflagellate cysts in recent sediments from the West Coast of Sweden. Bot. Mar. 43, 69-79.

Rochon, A., de Vernal, A., Turon, J.L., Matthiessen, J., Head, M.J., 1999. Distribution of Recent Dinoflagellate cysts in surface sediments from the North Atlantic Ocean and adjacent seas in relation to sea-surface parameters. Am. Assoc. of Stratigr. Palynol. AASP Contr. Ser. 35, 1-152.

1038 Rogerson, M., Rohling, E.J., Weaver, P.P.E., Murray, J.W., 2004. The Azores Front since the
1039 Last Glacial Maximum. Earth and Planetary Science Letters 222, 779-789.
1040
1041 Rogerson, M., et al., 2010. Enhanced Mediterranean-Atlantic exchange during Atlantic
1042 freshening phases, Geochem. Geophys. Geosyst. 11, Q08013, doi:10.1029/2009GC002931.
1043
1044 Rogerson, M., Schönfeld, J., Leng, M.J., 2011. Qualitative and quantitative approaches in
1045 palaeohydrography: A case study from core-top parameters in the Gulf of Cadiz. Marine Geology
1046 280 (1-4), 150-167.
1047
1048 Rogerson, M., Rohling, E.J., Bigg, G.R., Ramirez., J., 2012. Paleoceanography of the
1049 Atlantic-Mediterranean exchange: overview and first quantitative assessment of climatic
1050 forcing. Rev. Geophys. 50, RG2003, doi: 10.1029/2011RG000376.
1051
1052 Rohling, E.J., Hilgen, F.J., 1991. The eastern Mediterranean climate at times of sapropel
1053 formation: a review. Geol. Mijnb. 70, 253-264.
1054
1055 Rohling, E.J., Abu-Zied, R., Casford, C.S.L., Hayes, A., Hoogakker, B.A.A., 2009. The
1056 Mediterranean Sea: Present and Past. In: Physical Geography of the Mediterranean Basin. Oxford
1057 Regional Environments. Oxford University Press, 592 pp.
1058
1059 Rossignol-Strick, M., 1983. African monsoons, an immediate climate response to orbital
1060 insolation. Nature 30, 446-449.
1061

1062 Rudnick, D.L., 1996. Intensive surveys of the Azores Front: 2. Inferring the geostrophic and
1063 vertical velocity fields. Journal of Geophysical Research 101 (C7), 16,291-16,303.
1064
1065 Rüggeberg, A., Dullo, W.C., Dorschel, B., Hebbeln, D., 2007. Environmental changes and
1066 growth history of a cold-water carbonate mound (Propeller Mound, Porcupine Seabight). Int. J.
1067 Earth Sci. 96, 57-72.
1068
1069 Sabine, C.L., Feely, R.A., Watanabe, Y.W., Lamb, M., 2004. Temporal evolution of the North
1070 Pacific CO2 uptake rate. Journal of Oceanography 60 (3), 5-15.
1071
1072 Salgueiro, E., Voelker, A.H.L., de Abreu, L., Abrantes, F., Meggers, H., Wefer, G., 2010.
1073 Temperature and productivity changes off the western Iberian margin during the last 150 ky.
1074 Quaternary Science Reviews 29, 680-695.
1075
1076 Salgueiro, E., Naughton, F., Voelker, A.H.L., de Abreu, L., Alberto, A., Rossignol, L., Duprat, J.,
1077 Magalhães, V.H., Vaqueiro, S., Turon, J.L., Abrantes, F., 2014. Past circulation along the western
1078 Iberian margin: a time slice vision from the Last Glacial to the Holocene.Quat. Sci. Rev. 106,
1079 316-329.
1080
1081 Sánchez-Goñi, M.F., Turon, J.L., Eynaud, F., Gendreau, S., 2000. European climatic response to
1082 millennial-scale changes in the atmosphere-ocean system during the Last Glacial Period. Quat.
1083 Res. 54, 394-403.
1084
1085 Sánchez-Goñi, M.F., Cacho, I., Turon, J.L., Guiot, J., Sierro, F., Peypouquet, J.P., Grimalt, J.O.,
1086 Shackleton, N.J., 2002. Synchronicity between marine and terrestrial responses to millennial

scale climatic variability during the last glacial period in the Mediterranean region. Climate Dynamics 19 (1), 95-105.

Sánchez-Goñi, M., Landais, A., Fletcher, W., Naughton, F., Desprat, S., Duprat, J., 2008. Contrasting impacts of Dansgaard-Oeschger events over a western European latitudinal transect modulated by orbital parameters. Quaternary Science Reviews 27 (11-12), 1,136-1,151.

Sánchez-Goñi, M., Landais, A., Cacho, I., Duprat, J., Rossignol, L., 2009. Contrasting intrainterstadial climatic evolution between high and middle North Atlantic latitudes: A close-up of Greenland Interstadials 8 and 12. Geochem. Geophys. Geosyst. 10, Q04U04, doi:10.1029/2008GC002369.

Sánchez-Goñi, M.F., Harrison, S.P., 2010. Millennial-scale climate variability and vegetation changes during the Last Glacial: Concepts and terminology. Quaternary Science Reviews 29 (21-22), 2,823-2,827.

Sarmiento, J.L., Gruber, N., 2002. Sinks for anthropogenic carbon. Physics Today 55 (8). DOI: http://dx.doi.org/10.1063/1.1510279.

Schmittner, A., 2005. Decline of the marine ecosystem caused by a reduction in the Atlantic overturning circulation. Nature 434, 628-633.

Sierro, F.J., Hodell, D.A., Curtis, J.H., Flores, J.A., Reguera, I., Colmenero-Hidalgo, E., Barcena, M.A., Grimalt, J.O., Cacho, I., Frigola, J., Canals, M., 2005. Impact of iceberg melting on

Mediterranean thermohaline circulation during Heinrich events. Paleoceanography 20, PA2019, 1-13.

Sprangers, M., Dammers, N., Brinkhuis, H., van Weering, T.C.E., Lotter, A.F., 2004. Modern organic-walled dinoflagellate cyst distribution offshore NW Iberia; tracing the upwelling system. Review of Palaeobotany and Palynology 128, 97-106.

Stockmarr, J., 1971. Tablets with spores used in absolute pollen analysis. Pollen et Spores 13, 615-621.

Svensson, A., et al., 2008. A 60 000 year Greenland stratigraphic ice core chronology. Clim. Past 4, 47-57, doi:10.5194/cp-4-47-2008.

Takahashi, T., Sutherland, S.C., Wanninkhof, R., Sweeney, C., Feely, R.A., Chipman, D.W., Hales, B., Friederich, G., Chavez, F., Sabine, C., Watson, A., Bakker, D.C.E., Schuster, U., Metzl, N., Yoshikawa-Inoue, H., Ishii, M., Midorikawa, T., Nojiri, Y., Körtzinger, A., Steinhoff, T., Hoppema, M., Olafsson, J., Arnarson, T.S., Tilbrook, B., Johannessen, T., Olsen, A., Bellerby, R., Wong, C.S., Delille, B., Bates, N.R., de Baar, H.J.W., 2009. Climatological mean and decadal change in surface ocean pCO2, and net sea-air CO2 flux over the global oceans. Deep-Sea Research II 56 (8-10), 554-577.

Targarona, J., Warnaar, J., Boessenkool, K.P., Brinkhuis, H., Canals, M., 1999. Recent dinoflagellate cyst distribution in the North Canary Basin, NW Africa. Grana 38, 170-178.

1135 Toucanne, S., Mulder, T., Schönfeld, J., Hanquiez, V., Gonthier, E., Duprat, J., Cremer, M.,
1136 Zaragosi, S., 2007. Contourites of the Gulf of Cadiz: A high-resolution record of the
1137 paleocirculation of the Mediterranean outflow water during the last 50,000 years.
1138 Palaeogeography, Palaeoclimatology, Palaeoecology 246 (2-4), 354-366.
1139
1140 Toucanne, S., Jouet, G., Ducassou, E., Bassetti, M.A., Dennielou, B., Minto'o, C.M.A, Lahmi,
1141 M., Touyet, N., Charlier, K., Lericolais, G., Mulder, T., 2012. A 130,000-year record of levantine
1142 intermediate water flow variability in the Corsica Trough, western Mediterranean Sea. Quat. Sci.
1143 Rev. 33, 55-73.
1144
1145 Toucanne, S., Angue Minto'o, C.M., Fontanier, C., Bassetti, M.A., Jorry, S.J., Jouet, G., 2015.
1146 Tracking rainfall in the northern Mediterranean borderlands during sapropel deposition.
1147 Quaternary Science Reviews, in press.
1148
1149 Tuenter, E., Weber, S.L., Hilgen, F.J., Lourens, L.J., 2003. The response of the African summer
1150 monsoon to remote and local forcing due to precession and obliquity. Glob. Planet. Change 36,
1151 219-235.
1152
1153 Turon, J. L., 1984. Le palynoplancton dans l'environnement actuel de l'Atlantique Nord-oriental.
1154 Evolution climatique et hydrologique depuis le dernier maximum glaciaire. Mémoires de l'Institut
1155 de Géologie du Bassin d'Aquitaine 17, 313 pp.
1156
1157 Turon, J.L., Londeix, L., 1988. Les asssemblages de kystes de dinoflagellés en Méditerranée
1158 occidentale (Mer d'Alboran): mise en evidence de l'évolution des paléoenvironnement depuis le
1159 dernier maximum glaciaire. Bull. Centres Rech. Explor.-prod. Elf-Aquitaine 12, 313-344.

Turon, J.L., Lézine, A.M., Denèfle, M., 2003. Land-sea correlations for the last glaciation inferred from a pollen and dinocyst record from the Portuguese margin. Quaternary Research 59, 88-96.

Vautravers, M.J., Shackleton, N.J., 2006. Centennial-scale surface hydrology off Portugal during marine isotope stage 3: Insights from planktonic foraminiferal fauna variability. Paleoceanography 21, PA3004, doi:10.1029/2005PA001144.

Versteegh, G.J.M., 1994. Recognition of cyclic and non-cyclic environmental changes in the Mediterranean Pliocene; a palynological approach. Mar. Micropaleontol. 23, 147-171.

Vink, A., Zonneveld, K.A.F., Willems, H., 2000. Organicwalled dinoflagellate cysts in western equatorial Atlantic surface sediments: distributions and their relation to environment. Rev. Palaeobot. Palynol. 112, 247-286.

Voelker, A.H.L., Lebreiro, S.M., Schönfeld, J., Cacho, I., Erlenkeuser, H., Abrantes, F., 2006. Mediterranean outflow strengthening during northern hemisphere coolings: A salt source for the glacial Atlantic? Earth and Planetary Science Letters 245 (1-2), 39-55.

Voelker, A.H.L., de Abreu, L., Schönfeld, J., Erlenkeuser, H., Abrantes, F., 2009. Hydrographic Conditions Along the Western Iberian Margin During Marine Isotope Stage 2. Geochem. Geophys. Geosyst. 10(Q12U08), DOI: 10.1029/2009GC002605.

Voelker, A.H.L., Salgueiro, E., Rodrigues, T., Jimenez-Espejo, F.J., Bahr, A., Alberto, A., Loureiro, I., Padilha, M., Rebotima, A., Röhl, U., 2015. Mediterranean Outflow and surface water variability off southern Portugal during the early Pleistocene: A snapshot at Marine Isotope Stages 29 to 34 (1020–1135 ka). Global and Planetary Change 133, 223-237.

Waelbroeck, C., Labeyrie, L., Michel, E., Duplessy, J.C., McManus, J.F., Lambeck, K., Balbon, E., Labracherie, M., 2002. Sea-level and deep water temperature changes derived from benthic foraminifera isotopic records. Quaternary Science Reviews 21 (1-3), 295-305.

Wall, D., Dale, B., 1973. Paleosalinity relationships of dinoflagellates in the Late Quaternary of the Black Sea - A summary. Geosci. Man 7, 95-102.

Wall, D., Dale, B., Lohmann, G.P., Smith, W.K., 1977. The environment and climatic distribution of dinoflagellate cysts in modern marine sediments from regions in the north and south Atlantic oceans and adjacent seas. Mar. Micropaleontol. 2, 121-200.

Warrick, J.A., Fong, D.A., 2004. Dispersal scaling from the world's rivers. Geophysical research letters 31, L04301, doi:10.1029/2003GL019114.

Wienberg, C., Hebbeln, D., Fink, H.G., Mienis, F., Dorschel, B., Vertino, A., López Correa, M., Freiwald, A., 2009. Scleractinian cold-water corals in the Gulf of Cádiz – first clues about their spatial and temporal distribution. Deep Sea Res. I 56, 1873-1893.

1207 Wienberg, C., Frank, N., Mertens, K.N., Stuut, J.B., Marchant, M., Fietzke, J., Mienis, F., and
1208 Hebbeln, D., 2010. Glacial cold-water coral growth in the Gulf of Cádiz: Implications of
1209 increased palaeo-productivity: Earth and Planetary Science Letters. 298, 405-416.
1210
1211 Wolff, E.W., Chappellaz, J., Blunier, T., Rasmussen, S.O., Svensson, A., 2010. Millennial-scale
1212 variability during the last glacial: The ice core record. Quat. Sci. Rev. 29, 2828-2838.
1213
1214 Zanchetta, G., Drysdale, R.N., Hellstrom, J.C., Fallick, A.E., Isola, I., Gagan, M.K., Pareschi,
1215 M.T., 2007. Enhanced rainfall in the Western Mediterranean during deposition of sapropel S1:
1216 stalagmite evidence from Corchia cave (Central Italy). Quat. Sci. Rev. 26 (3-4), 279-286.
1217
1218 Zaragosi, S., Eynaud, F., Pujol, C., Auffret, G.A., Turon, J.L., Garlan, T., 2001. Initiation of
1219 European deglaciation as recorded in the north-western Bay of Biscay slope environments
1220 (Meriadzek Terrace and Trevelyan Escarpment): a multi-proxy approach. Earth Planet. Sci. Lett.
1221 188, 493-507.
1222
1223 Zonneveld, K.A.F., Ganssen, G., Troelstra, S., Versteegh, G.J.M., Visscher, H., 1997a.
1224 Mechanisms forcing abrupt fluctuations of the Indian Ocean summer monsoon during the last
1225 deglaciation. Quat. Sci. Rev. 16, 187-201.
1226
1227 Zonneveld, K.A.F., Versteegh, G.J.M., De Lange, G.J., 1997b. Preservation of organic walled
1228 dino£agellate cysts in di¡erent oxygen regimes: a 10,000 years natural experiment. Mar.
1229 Micropaleontol. 29, 393-405.
1230

1231 Zonneveld, K.A.F., Hoek, R.P., Brinkhuis, H., Willems, H., 2001. Geographical distributions of
1232 organic-walled dinoflagellate cysts in surficial sediments of the Benguela upwelling region and
1233 their relationship to upper ocean conditions. Progress in Oceanography 48, 25-72.
1234
1235 Zonneveld, K.A.F, Marret, F., Versteegh, G.J.M., Bogus, K., Bonnet, S., Bouimetarhan, I.,
1236 Crouch, E., de Vernal, A., Elshanawany, R., Edwards, L., Esper, O., Forke, S., Grøsfjeld, K.,
1237 Henry, M., Holzwarth, U., Kielt, J.F., Kim, S.Y., Ladouceur, S., Ledu, D., Chen, L., Limoges, A.,
1238 Londeix, L., Lu, S.H., Mahmoud, M.S., Marino, G., Matsouka, K., Matthiessen, J., Mildenhal,
1239 D.C., Mudie, P.J., Neil, H.L., Pospelova, V., Qi, Y., Radi, T., Richerol, T., Rochon, A.,
1240 Sangiorgi, F., Solignac, S., Turon, J.L., Verleye, T., Wang, Y., Wang, Z., Young, M., 2013. Atlas
1241 of modern dinoflagellate cyst distribution based on 2405 data points. Review of Palaeobotany
1242 and Palynology, 191, 1-197.
1243
1244

Biogeosciences Discuss., doi:10.5194/bg-2016-144, 2016
Manuscript under review for journal Biogeosciences
Published: 21 April 2016

1245 **9. TABLE CAPTION**

1246

1247 **Table 1**: Modern distribution versus past occurrences (MD99-2339 record) for selected major
1248 dinocyst species found in the fossil assemblage (cf. Figure 5).

1249

1250 **10. FIGURE CAPTION**

1251

1252 **Figure 1:** Area of interest with major sea-surface features. Study core MD99-2339, as well as
1253 other cores discussed in the paper, are located on the large map, depicting also the bathymetry of
1254 the study area and the major surface currents within the Alboran sea; WAG: Western Alboran
1255 Gyre; EAG: Eastern Alboran Gyre; AOF: Almeria-Oran Front; AC: Algerian Current. The small
1256 map on the left present large scale North-Atlantic currents with: the North Atlantic Drift (NAD),
1257 the Portugal Current (PC) flowing southward from 45°N to 30°N, the Azores Current (AzC)
1258 derived from the southern branch of the Gulf Stream and flowing eastward to the Gulf of Cadiz at
1259 about 35°N, and the Canary Current (CC) fed by both the AzC and the PC. Together, these
1260 currents form the Eastern Boundary Current of the North Atlantic subtropical gyre.

1261

1262 **Figure 2:** Comparison, against age (new age model from this study), between the planktonic
1263 $\delta^{18}O$ monospecific record of core MD99-2339 (red curve, Voelker et al., 2006) and the NGRIP
1264 $\delta^{18}O$ according to the GICC05 timescale (Svensson et al., 2008). a) Red stars locate the 6
1265 radiocarbon dates retained for the chronology of core MD99-2339, and dark arrows locate the 13
1266 pointers used to tune the $\delta^{18}O$ data of core MD99-2339 to the NGRIP chronology, by considering
1267 onset of GI (numbers 1 to 12 on the Figure) according to Wolff et al. (2010). Sedimentation rates
1268 calculated between different pointers of core MD99-2339 are also highlighted with the dark

1269 histogram. YD: Younger Dryas, BA: Bölling-Alleröd. b) A zoom on the interval 25-50 ka BP
1270 enables to better consider the pointers selected (dotted vertical lines) for this new age model.
1271
1272 **Figure 3:** Depth-age model for core MD99-2339 (all symbols are explained in the Figure, cf. also
1273 Figure 2), allowing to compare the new age model (this study, planktonic $\delta^{18}O$ monospecific
1274 record in black) with the first published one (Voelker et al., 2006, planktonic $\delta^{18}O$ record in red).
1275
1276 **Figure 4:** Data from core MD99-2339 against depth (cm). $\delta^{18}O$ planktonic monospecific record
1277 of core MD99-2339 (a, Voelker et al., 2006), is presented in parallel with the W/C qualitative
1278 index of surface temperatures (b). Diversity indexes (species richness according to the Margalef
1279 index, c, and dominance, d) are drawn in parallel with percentages of the major species *L.*
1280 *machaerophorum* (e). Different calculations of dinocyst concentrations (f, g) are represented in
1281 linear scale, while h) illustrates total dinocyst and *L. machaerophorum* concentrations in
1282 logarithmic scale, compared with sedimentation rates (i) and dinocyst fluxes (j). GI: Greenland
1283 Interstadial. Grey bands indicate Heinrich Stadials (HS) and the Younger Dryas (YD).
1284
1285 **Figure 5:** Data from core MD99-2339 against age (cal ka BP): major taxa occurring with values
1286 higher than 2% in dinocyst assemblages from MD99-2339 core (0-48 ka BP; 0-1,854cm). Red,
1287 blue and green colours respectively indicate the "Warm", "Cold", and "Heterotrophic" groups.
1288 W/C: Warm-Cold Ratio. The trends shown in grey are calculated by excluding *Lingulodinium*
1289 *machaerophorum* from the main dinocyst sum, while coloured curves (colors explained in the
1290 Figure) depict the whole assemblage considering all species. MD04-2805 CQ dinocyst data are
1291 also represented over the 28 ky BP so as to illustrate similarities between the assemblages from
1292 the central (MD99-2339, this study) and southern (MD04-2805 CQ; Penaud et al., 2011a) Gulf of

Biogeosciences Discuss., doi:10.5194/bg-2016-144, 2016
Manuscript under review for journal Biogeosciences
Published: 21 April 2016

1293 Cadiz. Pink bands indicate warmer intervals (including: BA: Bölling-Alleröd, LGM: Last Glacial
1294 Maximum, GI: Greenland Interstadial) and blue bands indicate colder events (HS: Heinrich
1295 Stadials and YD: Younger Dryas).
1296
1297 **Figure 6:** Data from core MD99-2339 against age (cal ka BP). $\delta^{18}O$ planktonic monospecific
1298 record and *N. pachyderma* s. percentages from core MD99-2339 (Voelker et al., 2006) in parallel
1299 with dinocyst transfer function results (n= 1492; Radi and de Vernal, 2008) : Winter and Summer
1300 Sea Surface Temperature (SST) and Sea Surface Salinity (SSS), as well as Seasonality (SST
1301 summer - SST Winter) and Annual Productivities. Total dinocyst and heterotrophic fluxes are
1302 also depicted with the ratio H/A for "Heterotrophics/Autotrophics", and percentages of two
1303 species: *L. machaerophorum* as a species index for higher surface stratification linked with
1304 increased paleo-river discharges and *B. tepikiense* as a species index for thermal seasonal
1305 contrasts. Stars on each graph indicate present-day values for the different surface hydrological
1306 parameters and dinocyst percentages recorded in modern sediments.
1307
1308 **Figure 7:** Greenland $\delta^{18}O$ data (a) over the last 50 ky in parallel with $\delta^{18}O$ data (b) and grain-size
1309 analysis from core MD99-2339 (c). Dinocyst data (f, h, i, j) from core MD99-2339 are also
1310 depicted versus Western (pollen, Alboran Sea, g) and Eastern ($\delta^{18}O$, Soreq Cave, m)
1311 Mediterranean records, as well as orbital parameters (d, e). Sedimentation rates (l) calculated
1312 from new age model of core MD99-2339 echoe total dinocyst concentrations (k) over the last 50
1313 ky. Greenland Interstadials (GI) 1 (Bölling-Alleröd: BA), 8 and 12 are highlighted with yellow
1314 bands and are characterized by a bipartite structure labelled "a" and "b" for the first and second
1315 phases, respectively. Grey bands indicate Heinrich Stadials (HS) and the Younger Dryas (YD).
1316 Orange vertical band indicates the time interval corresponding to sapropel 1 (S1) formation (9.5-

Biogeosciences Discuss., doi:10.5194/bg-2016-144, 2016
Manuscript under review for journal Biogeosciences
Published: 21 April 2016

6.5 ka BP).

Figure 8: Comparison between dinocyst data (in percentages or absolute concentrations) as recorded from each side of the Strait of Gibraltar. Full blue / blue curves represent MD99-2339 data (Gulf of Cadiz, this study) while full red / red curves represent MD95-2043 data (Alboran Sea, Penaud et al., 2011b). Greenland Interstadials (GI) 8 and 12 are highlighted with yellow bands and are characterized by a bipartite structure labelled “a” and “b” for the first and second phases, respectively. Other GI are highlighted with pink bands also corresponding to the numbered peaks obvious on the NGRIP curve. Grey bands indicate Heinrich Stadials (HS).

Biogeosciences Discuss., doi:10.5194/bg-2016-144, 2016
Manuscript under review for journal Biogeosciences
Published: 21 April 2016

1327 See Supplement Material for Table 1

1328

1329

1330

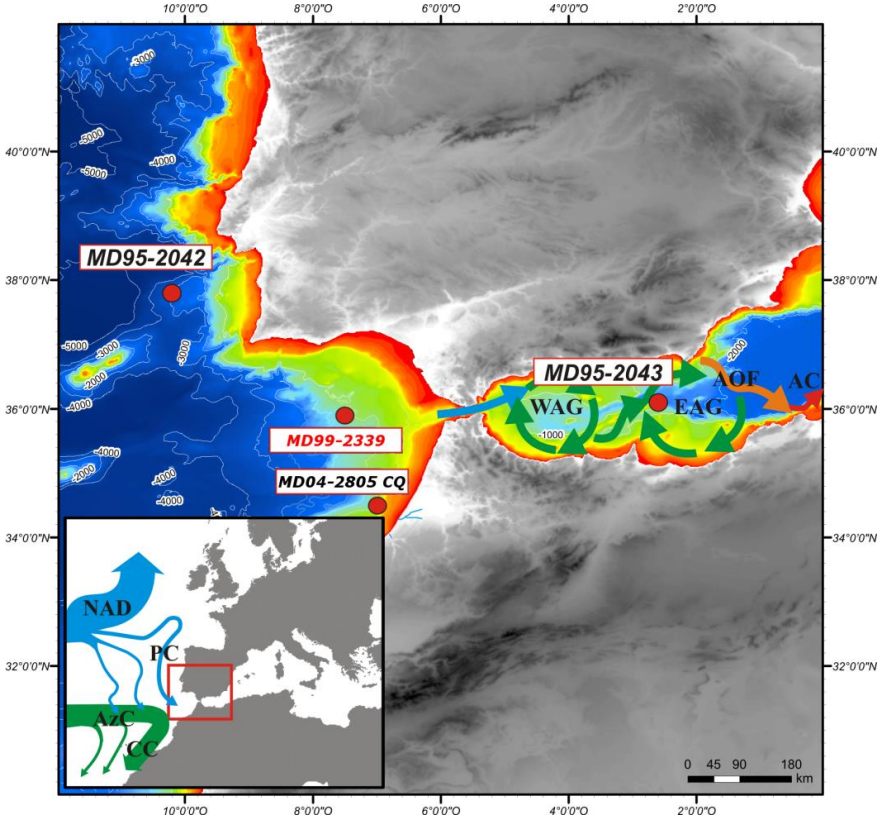

1331

1332

1333 Figure 1

1334

Biogeosciences Discuss., doi:10.5194/bg-2016-144, 2016
Manuscript under review for journal Biogeosciences
Published: 21 April 2016

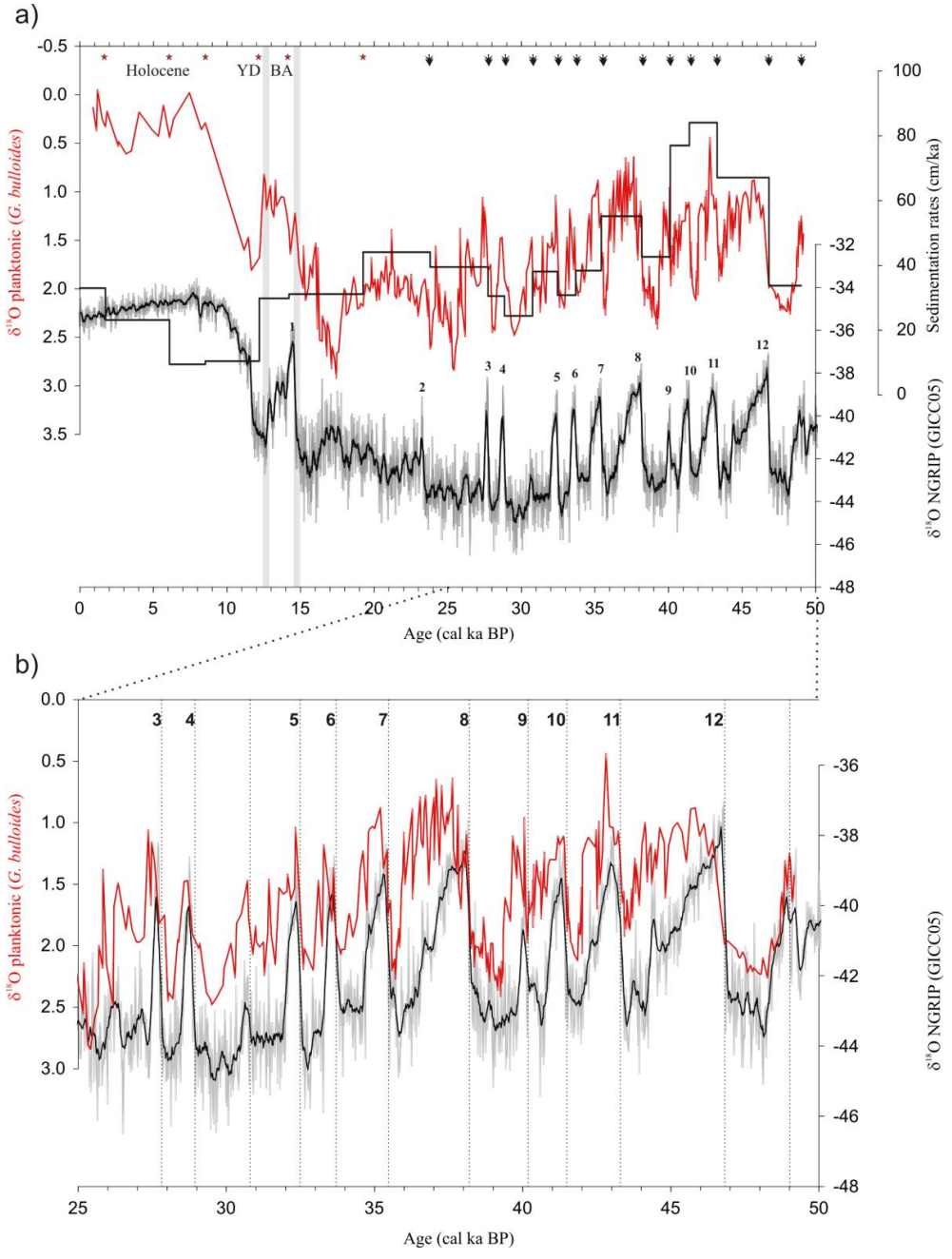

1335

1336 Figure 2

1337

Biogeosciences Discuss., doi:10.5194/bg-2016-144, 2016
Manuscript under review for journal Biogeosciences
Published: 21 April 2016

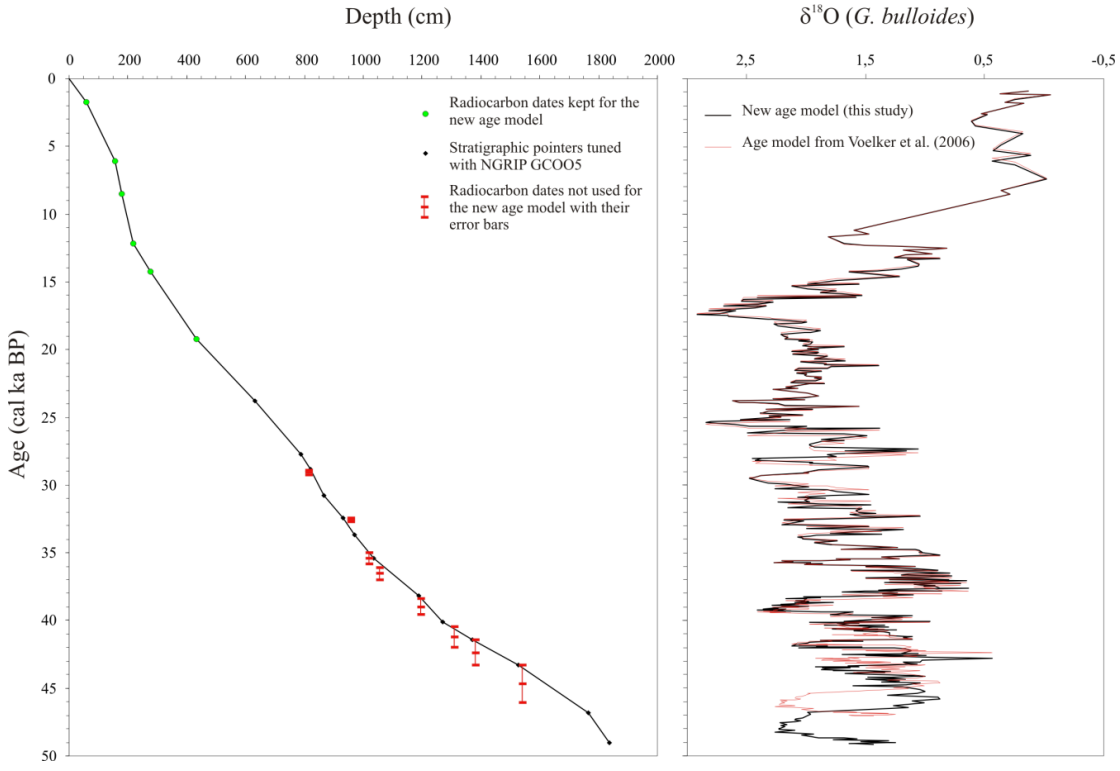

1338

1339 Figure 3

Biogeosciences Discuss., doi:10.5194/bg-2016-144, 2016
Manuscript under review for journal Biogeosciences
Published: 21 April 2016

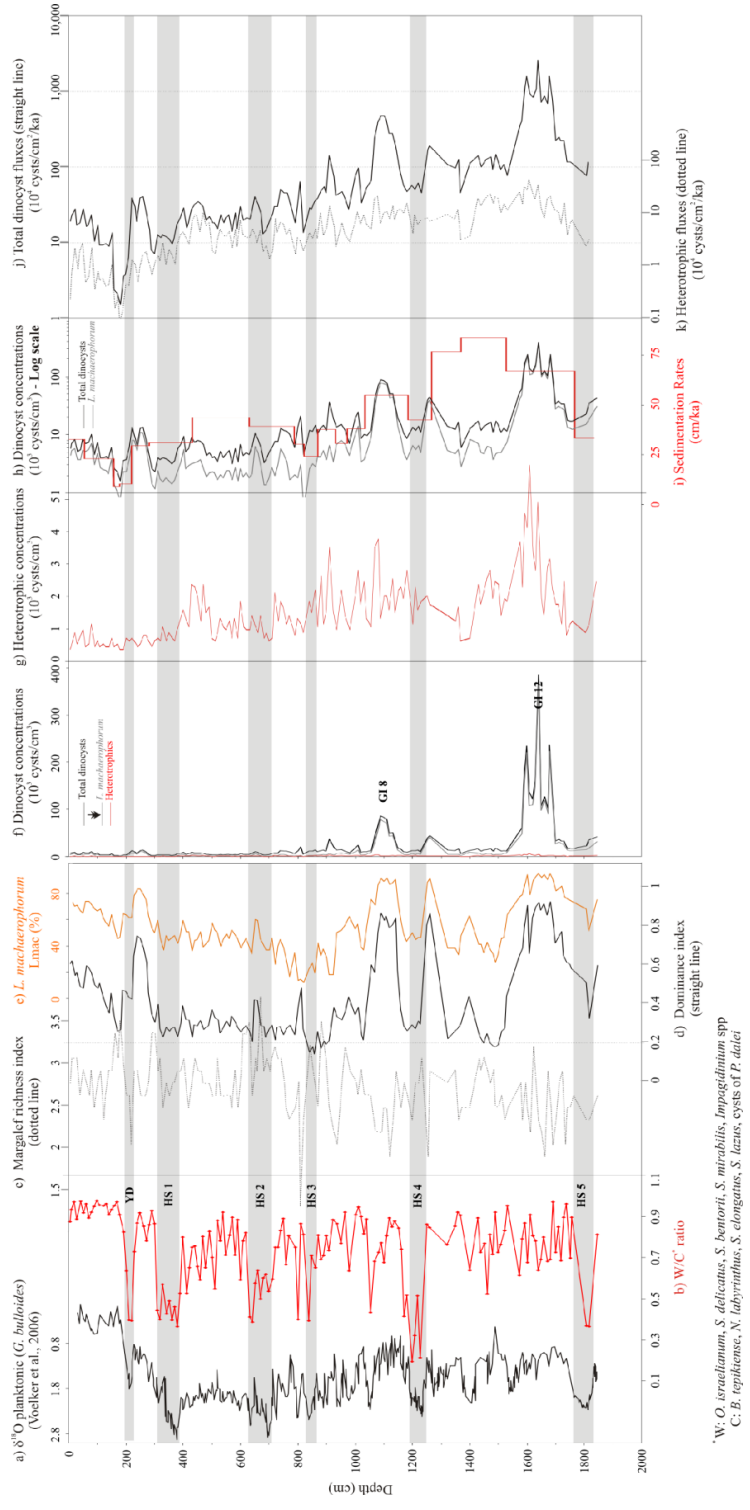

1340

1341 Figure 4

Biogeosciences Discuss., doi:10.5194/bg-2016-144, 2016
Manuscript under review for journal Biogeosciences
Published: 21 April 2016

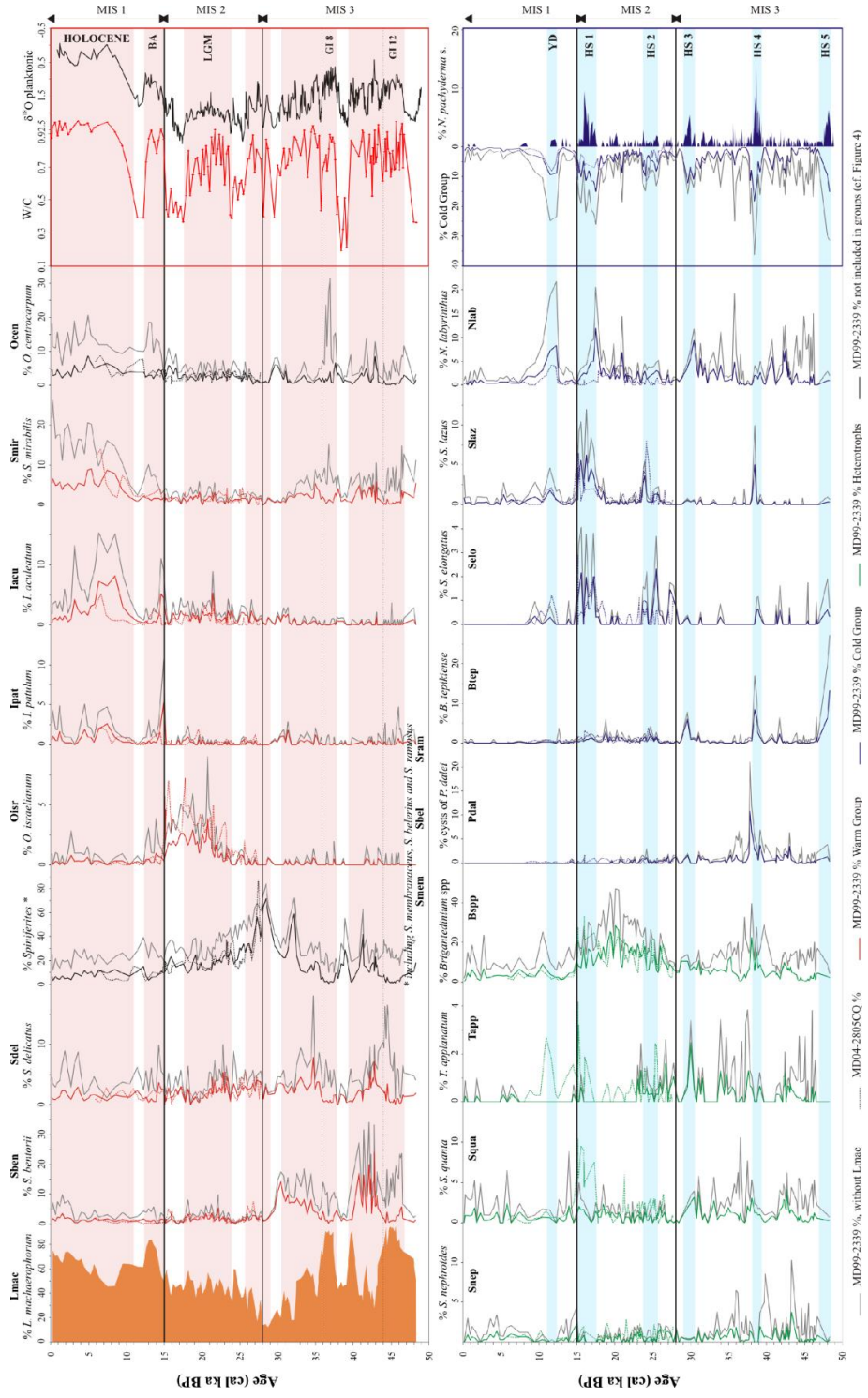

1342

1343 Figure 5

Biogeosciences Discuss., doi:10.5194/bg-2016-144, 2016
Manuscript under review for journal Biogeosciences
Published: 21 April 2016

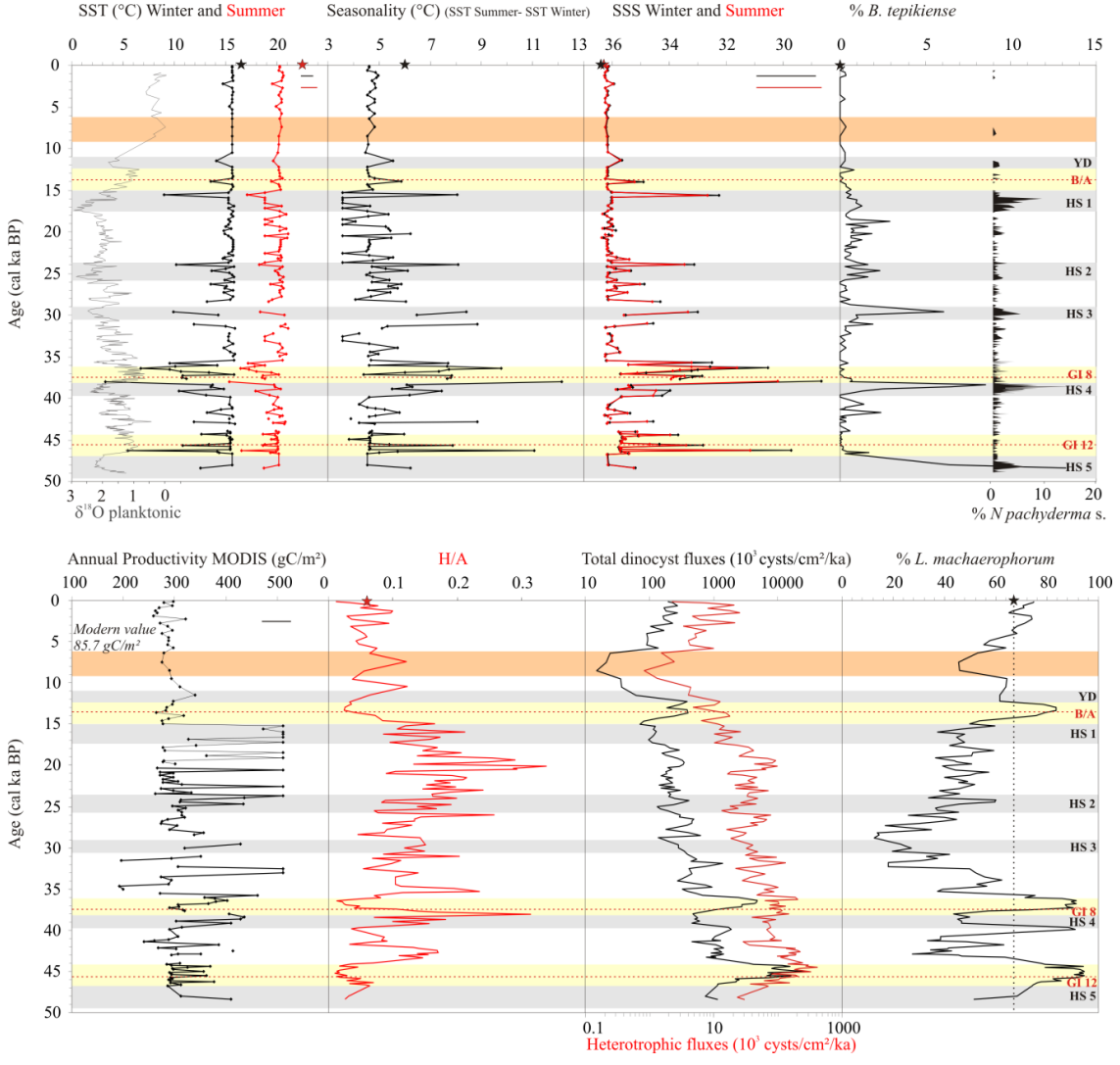

1344

1345 Figure 6

1346

Biogeosciences Discuss., doi:10.5194/bg-2016-144, 2016
Manuscript under review for journal Biogeosciences
Published: 21 April 2016

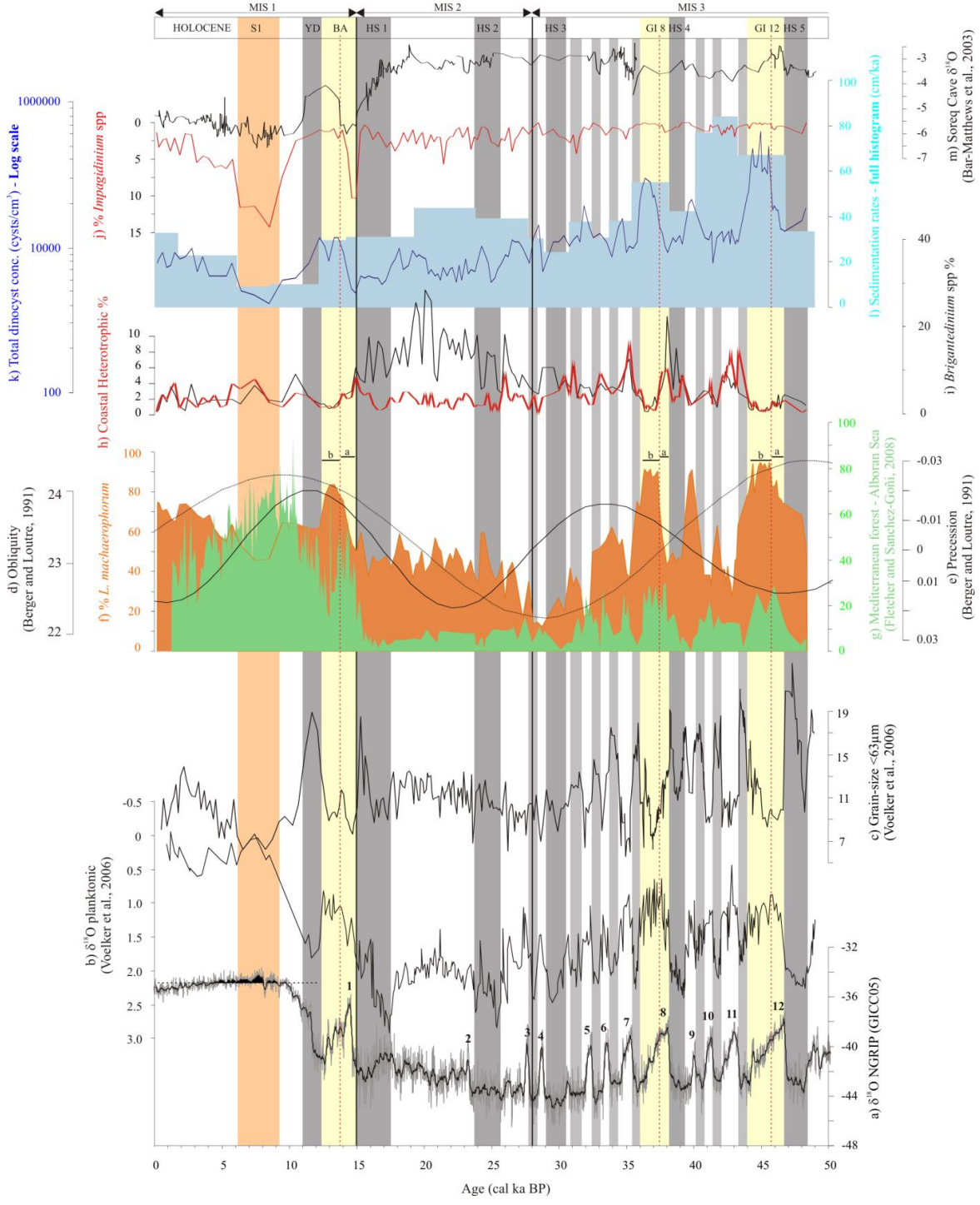

1347

1348 Figure 7

Biogeosciences Discuss., doi:10.5194/bg-2016-144, 2016
Manuscript under review for journal Biogeosciences
Published: 21 April 2016

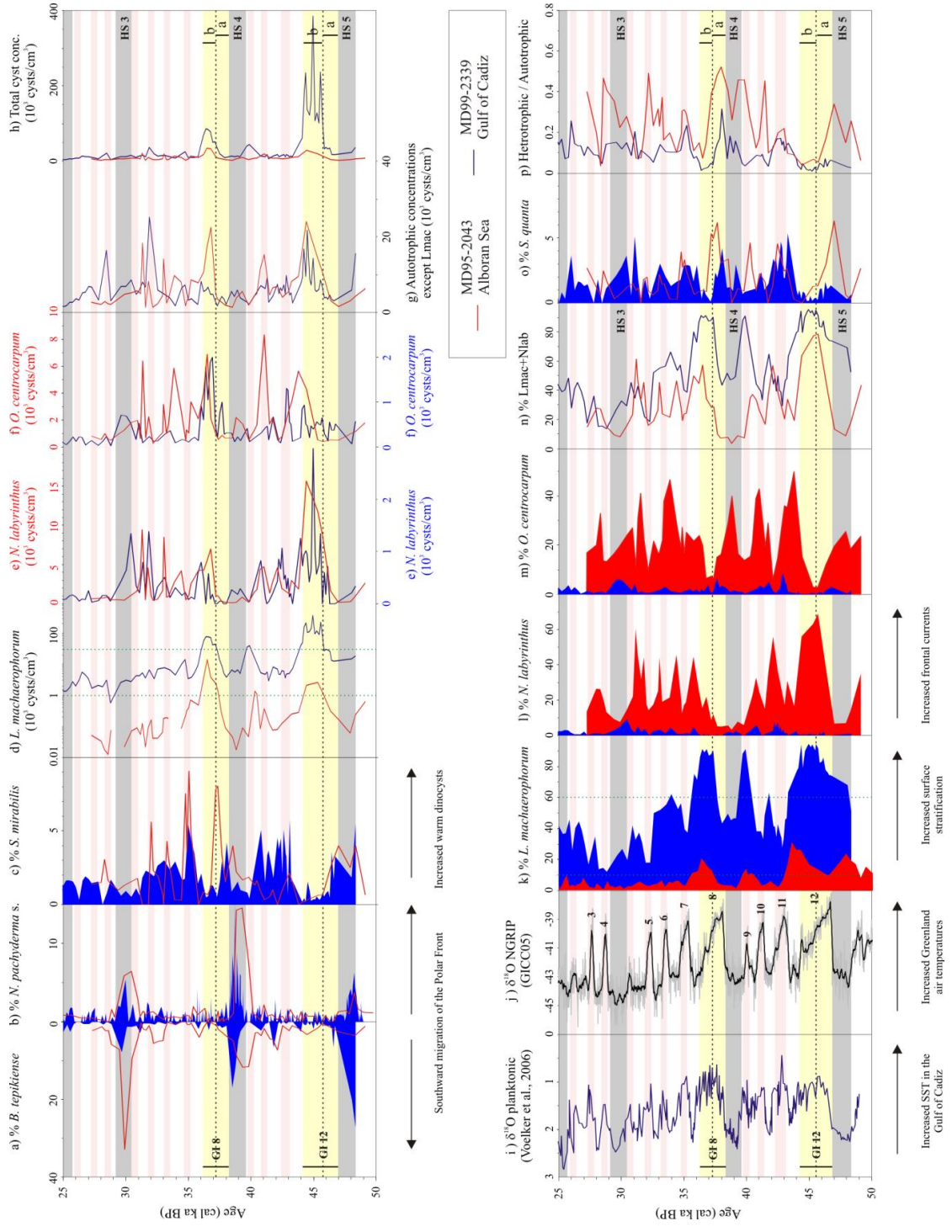

1349

1350 Figure 8